Summer 2020

In Silico Investigation for the Conversion of Methyl Oleate to Gasoline

Arkanil Roy
Missouri State University, Roy160509@live.missouristate.edu

IN SILICO INVESTIGATION FOR THE CONVERSION OF METHYL OLEATE TO GASOLINE

A Master's Thesis

Presented to

The Graduate College of

Missouri State University

In Partial Fulfillment

Of the Requirements for the Degree

Master of Science, Chemistry

By

Arkanil Roy

August 2020

***IN SILICO* INVESTIGATION FOR THE CONVERSION OF BIODIESEL TO GASOLINE**

Chemistry

Missouri State University, August 2020

Master of Science

Arkanil Roy

ABSTRACT

Petroleum products are found in all walks of life. From the plastic casing on a cell phone to the gasoline that runs most vehicles, a lot is derived from petroleum. Ubiquitous use of petroleum has adversely affected the environment. Toxic substances such as SO_x and NO_x are released into the atmosphere during the processing and usage of petroleum products, which contributes to global warming. Inevitable oil spills cause devastating effects to marine ecosystems. The rate of regeneration of petroleum is much slower than the rate of usage that would lead to it being exhausted in the recent future. Hence, a more sustainable and ecological source of energy is needed. Biodiesels are one of the common sources of alternate fuel. They are mainly composed of Fatty Acid Methyl Esters (FAMEs) and are synthesized by transesterification of triglycerides found in various food oils for example soybean oil and canola oil in presence of methanol. Biodiesels claim some advantages over conventional fuels namely lower SO_x and CO_2 emissions, high flash point and cetane number, biodegradable characteristics and non-toxic nature. But there are various disadvantages to it as well. FAMEs have higher NO_x emission than petroleum fuel, they gel at temperatures routinely reached in the United States (leading to clogged fuel filters), they dislodge previously deposited carbon due to surfactant properties, and they are more expensive to produce. A solution to usability of FAMEs is pyrolysis or thermal cracking. Pyrolysis or thermal cracking into smaller compounds that include petroleum products like plastic precursors and gasoline. Simulations at the (DFT) M06-2X/6-31G+(d,p) level of theory show promising correlation to experimental work. Herein, the FAME methyl oleate is studied. Methyl oleate is the most abundant FAME in canola oil, the largest source of biodiesel in Europe. Results from the simulations show formation of long alkyl chains, some containing a free radical, carbon monoxide and cyclic products including 3-membered rings.

KEYWORDS: petroleum, biodiesel, pyrolysis, DFT, Ergodicity, molecular dynamics, simulation, computation

IN SILICO INVESTIGATION FOR THE CONVERSION OF BIODIESEL TO GASOLINE

By

Arkanil Roy

A Master's Thesis
Submitted to the Graduate College
of Missouri State University
In Partial Fulfillment of the Requirements
For the Degree of Master of Science, Chemistry

August 2020

Approved:

Matthew R. Siebert, Ph.D., Thesis Committee Chair

Richard Biagioni, Ph.D., Committee Member

Fei Wang, Ph.D., Committee Member

Gautam Bhattacharyya, Ph.D., Committee Member

Kartik Ghosh, Ph.D., Committee Member

Julie Masterson, Ph.D., Dean of the Graduate College

ACKNOWLEDGEMENTS

I would like to thank whole of Dr. Siebert's lab, especially Michael Bakker, who helped me get into the world of quantum chemistry. I would like to thank Dr. Matthew R. Siebert, without the assistance of whom, I would be struggling to understand quantum chemistry.

I would like to thank Dr. Gary Meints for teaching me quantum chemistry and helping me understand this subject better. I would like to thank my thesis committee for giving feedback and helping in making this thesis better. I would also like to thank members of the Department of Chemistry, especially Linda, who has always helped me in getting all the official things done and Dr. Schick for helping me making all academic decisions.

I would like to thank past and present graduate students of the Department of Chemistry, especially Alisson, Molly, Alex, Kevin, Luckio and Adjoa. They helped me keep sane and have fun during this tedious process.

Lastly, I would like to thank my parents for always supporting me and allowing me to do whatever I wanted to do and affirming to all decisions I take in life.

I dedicate this thesis to my parents.

TABLE OF CONTENTS

LIST OF TABLES

LIST OF FIGURES

CHAPTER 1: ALTERNATIVE FUEL

1.1 Petroleum and its uses

Petroleum products are one of the most used commodities in recent times. They are used in various walks of life, from transportation fuels (namely gasoline, diesel, airplane fuel, etc.) to lubricants and plastics. The versatility of petroleum makes it one of the most exploited natural resources in the world.[1] According to the US Energy Information Administration (EIA), in 2018 approximately 7.5 billion barrels of petroleum were used, of which, 46% was motor gasoline, 20% was distillate fuel and 8% was jet fuel. The remainder was converted into other petroleum products. [2]

Petroleum is a naturally occurring yellowish-black fluid formed from other plant and animal remains under intense geological pressure and heat. Petroleum consists of various hydrocarbons, traces of metals like vanadium, cobalt and nickel, napthenes and small percentages of oxygen, nitrogen and sulfur that affect the purity and quality of fuels after purification. [3]

1.2 Disadvantages of petroleum

In recent times, the use of petroleum is under controversy due to the adverse effects of the emissions on the environment that leads to global warming (increase in overall average temperature of the Earth) and ocean acidification (decrease in pH in Earth's oceans due to uptake of CO_2 from the atmosphere). [4, 5] Additionally, obtaining petroleum is a labor-intensive task and includes drilling to extract crude oil from wells, which has adverse effects on marine life due to

ecosystem interference. Oil spills also cause adverse effects on the ecosystem. Purification of petroleum fuel also requires a lot of work. [6]

1.3 Alternative Fuel

Alternative fuels are substitute sources of fuel to conventional fossil fuel. These are used to mitigate the disadvantages caused by fossil fuels. They are renewable and ecological and are gaining ground in the past few decades. Some of them are elaborated below.

1.3.1 Solar energy. Solar energy utilizes the radiant heat and light from the sun that is trapped using solar panels, photovoltaic cells, and artificial photosynthesis. [7] It is an important source of renewable energy and has attained great heights in the recent past. According to the United Nations Development Program in its 2000 World Energy Assessment, solar energy has a potential of producing 1,575 - 49,837 exajoules (EJ), which is larger than the total world consumption of 559.8 EJ in 2012. [8, 9] However, solar energy has some glaring disadvantages. Solar energy is expensive to set up and use, but with increasing technology it is becoming more affordable. It is also dependent on weather and cannot be used everywhere. The efficiency of conversion into solar energy from sunlight is low. [7] The biggest disadvantage of solar energy is that it is not usable in automotive sector, other than for charging of electric car batteries.

1.3.2 Wind energy. Wind energy utilizes air flow through turbines to provide mechanical power to charge generators. These generators would then provide power to the local power grid. Wind energy is one of the most ecologically friendly sources of energy as it has a very small impact on the environment. [10] According to the Global Wind Energy Council (GWEC), the global wind power capacity grew by 9.6% to 591gigawatts (GW) in 2018, suggesting the acceptance of wind energy. [11] However, big wind farms require a lot of space, as they need to be

more spread out than other energy plants. Since a large amount of space is needed, these farms are generally erected in rural areas, which leads to rural industrialization and habitat loss. Like solar energy, wind is also dependent on weather and can be inconsistent. It is expensive to set up, but is cost-effective in the long run. [12] Being a stationary power source, it is not usable as an automotive energy source.

1.3.3 Hydroelectricity. Hydroelectricity utilizes the energy of fast flowing or falling water, which can be harnessed using watermills and turbines. These watermills or turbines are connected to electric power transmissions and are used to power an energy grid that provides electricity to perform various tasks. Hydroelectricity has been around for a long time, since the late 19th century. [13] Hydroelectric plants can be classified into three parts based on units produced: large (>30 MW), small (100 kW-30 MW) and micro (<100 kW). Hydroelectricity is the largest contributor of all renewable energy sources and accounts for 6.7% of worldwide electricity production. [14] There are substantial concerns with hydroelectricity, the main of which is the environmental impact of dam construction. Construction of dams on rivers cause the disruption of the local ecosystem, floods upstream landscapes, blocks fish passages, and displaces local communities. Additionally, dam failures can be catastrophic for those who live downstream. [15]

1.3.4 Nuclear energy. Nuclear power uses the energy from nuclear reactions to produce heat, which is then used to steam water that rotate turbines to produce electricity. Nuclear power is generated from nuclear fission and nuclear decay. The most prevalent source of electricity through nuclear power is the fission between uranium or plutonium atoms. Nuclear power has attained a high position since 1970s. [16] In 2017, nuclear power provided 2,488 terawatt hours (TWh) of electricity, making it the second largest global alternative fuel source after

hydroelectricity. [17] Nuclear power has the lowest level of fatalities when compared to other alternative sources. [17] However, there are factors that make this energy source controversial. The most common radioactive element, uranium, has a tedious mining and refining process, causing pollution. Safe radioactive waste disposal is also an important concern. There is also tandem greenhouse gas production and accidents that occur during construction. Maintenance and construction are also expensive. The most crucial concern is nuclear accidents, like Chernobyl and Fukushima that has society reconsidering the safety of this process. [16]

1.3.5 Biofuels. Biofuel is produced by anthropogenic means using biomass as the source, rather than conventional fuel that is formed from older plant and animal remains converted geologically. Common examples of biofuels include ethanol, biodiesel and biogas. However, generally biomass refers to the organic raw material the fuel is manufactured from. [4, 18] Biofuel is regarded as transportation fuels made from organic material by the Energy Information Administration (EIA). Sources of biofuel include agricultural crops and biological wastes from various commercial, domestic and agricultural facilities. In 2018, global biofuel production increased by 7% from 2017, producing about 152 billion liters, according to Transport Biofuels. [19] Sources of biofuels make them cheaper to garner and boom local economies. They are taxed less than conventional fuel, adding to affordability. However, this also leads to competition for food crops and increase in the price of crops. The large amount of land used to harvest these sources decreases the amount of land for food. Due to mentioned factors, these fuels are also unusable at certain areas in the world. [20, 21]

1.3.5.1 Biodiesel. Out of all these alternate sources, biodiesel is very promising as an upcoming substitute to conventional automotive fuel. Biodiesel comprises 12-20 carbon monoalkyl chain fatty acid methyl esters (FAMEs), which are derived from cooking oils and

animal fats. FAMEs can be produced by a carbon neutral processes (photosynthesis) followed by transesterification. [4]

Biodiesels have certain advantages to conventional petroleum fuels. First, the process of manufacturing biodiesel is a more ecological method and does not affect the environment in the same way as petroleum. Second, biodiesel emissions are way less harmful to the environment as combustion of biodiesel contains fewer SO_x compounds, greenhouse gases such as CO_2, and soot particles. Also, since biodiesel is an active production process (source grown anthropogenically) they are not as fast depleting as that of petroleum. [4, 22-24] However, there are certain disadvantages as well. Emissions from biodiesels give out more NO_x compounds than petroleum fuels. Also, biodiesels are rendered useless in low temperature climates, as they gel, which can clog the engines and can cause complications/damage the engine of the vehicle. Modifying vehicles to exclusively suit use of biodiesel can be expensive, and hence more affordable and efficient methods are needed to make biodiesels more usable. [23, 25] One such process is pyrolysis.

Pyrolysis, or thermal cracking, is a process already utilized for the processing of petroleum. Using thermal cracking, FAMEs can be broken down into smaller products by exposure to high temperatures and pressure, which can then be marketed as fuels (mainly gasoline) and other necessary precursor products that include petroleum precursors. [4]

1.3.5.2 Sources and Manufacture of FAMEs. The synthesis of biodiesel involves transesterification of triglycerides with methanol, in presence of a catalyst, and the products formed are glycerol and FAMEs, as illustrated in Figure 1. The catalyst is generally an acid, base, or an enzyme. The FAMEs formed will depend on the alkyl groups present in the triglycerides. [4, 25, 26]

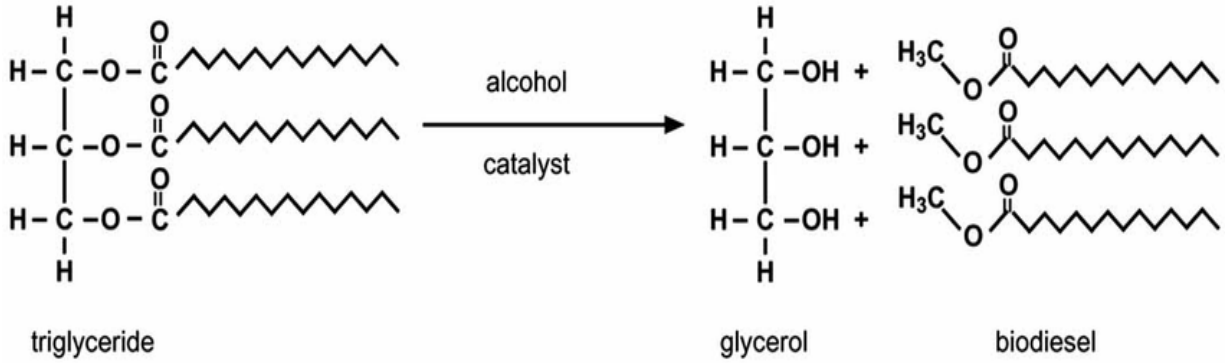

Figure 1. Transesterification of triglycerides with methanol, in the presence of catalyst, forming FAMEs and glycerol.

Food oils are triglycerides of fatty acids. Oleic acid is the largest constituent in canola oil, which is the largest source of biodiesel in Europe, and a major constituent in soybean oil, the largest source of biodiesel in USA. Oleic acid forms the fatty acid methyl ester, methyl oleate. It is an 18-carbon methyl ester with a single unsaturation. A list of common food oils and their fatty acids compositions are shown in Table 1.

Table 1. Composition of fatty acids in various food oils. [27]

Food Oils	Oleic Acid (18:1) (%)	Linoleic Acid (18:2) (%)	Linolenic Acid (18:3) (%)	Sat. Fatty Acid (%)
Canola	61.8	18.6	9.1	7.4
Soybean	22.6	51	7	15.6
Palm	40	9.1	0.2	49.3
Olive	71.3	9.8	0.7	13.8
Sunflower	19.5	65.7	0	10.3

1.3.6 Transesterification methods. One of the major concerns regarding transesterification is the large excess of methanol needed to shift the reaction equilibrium

towards the products. For better production of FAMEs in the widely used homogeneous phase alkaline-catalyzed method, oils with less than 0.5% free fatty acids (FFA) should be used. Higher FFA content causes ester saponification and catalyst consumption leading to a lower efficiency of the transformation. Another important factor for efficient conversion is low water content (less than 0.06%). Pre-treatments are sometimes done to solve the above problems, but they are expensive. [4, 28-29]

The production of biodiesel is very expensive, when compared to petroleum and other alternative fuels, owing to cost of the feedstock. Hence, waste cooking oils and animal fats are often used as more affordable sources of triglycerides. The biggest con of using these sources is high content of water (about 3%) and FFA (6%). [4, 26, 28-29]

1.3.6.1 Supercritical Method. Transesterification carried out under supercritical conditions (at temperatures and pressures higher than critical point of the mixture) can be an efficient alternative to catalysis. In this method, the mixture of methanol and oil becomes a single homogeneous phase, which removes the inhibition caused by interphase mass transfer (transfer of mass between two different phases due to difference in concentration at the interface). This method is more ecological due to lack of waste produced from catalyst treatment and separation of catalyst from final products. Pretreatment of the feed is not required as FFAs and water content do not affect a non-catalyzed reaction. [4, 26, 28-29]

There are certain disadvantages to this process. The high ratio of methanol to oil (40:1) makes it difficult to separate the methanol for reuse. Additionally, the high temperature and pressure (300-450 °C at 20 - 50 MPa for a yield of 95% in about 4 - 15 minutes) leads to a very high energy consumption which makes it less economical, when done at an industrial level. These severe conditions also bring concerns regarding the stability of biodiesel, as

polyunsaturated fatty acids are susceptible to reactive oxygen species. and vulnerable to alterations. [4, 26, 28-29]

To solve the above-mentioned issues, adding co-solvents such as carbon dioxide and propane, or adding heterogeneous catalysts such as calcium oxide into the reaction mixture, allows lower temperature, pressure, and alcohol equivalents required. [4, 26, 28-29]

1.3.6.2 Chemical Catalysts. Different catalysts vary the route of transesterification and the kinetics of the reaction. Chemical catalysts like acid and alkaline have shown to portray pseudo-first-order kinetics for butanol:soybean oil at 30:1 molar ratio. With alkaline catalysis the forward reaction follows consecutive second order kinetics for butanol:soybean oil at 6:1 molar ratio. [4, 26, 28-29]

1.3.6.2.1 Acid Catalysis. Acids generally used for catalysis are sulfuric, phosphoric, hydrochloric and organic sulfonic acids. Alkaline catalysis is generally faster than acid catalysis, but acid catalysis is required for glycerides that have high FFA and water content. It is observed that *in situ* transesterification reactions are more efficient than conventional reaction procedure. The difference between the two processes is that in *in situ* reaction, the oil-bearing material is mixed with acidified alcohol, contrary to adding oil that has been treated to alcohol. The alcohol acts as both an extracting agent as well as a catalyst, hence it is more efficient as extraction and transesterification in the same reaction. Various oils such as sunflower and rice bran oils have shown to give better yield under *in situ* conditions. [4, 26, 28-29]

1.3.6.2.2 Alkaline Catalysis. For alkaline catalysis, the common bases used are NaOH, KOH, carbonates and alkoxides such as sodium methoxide, sodium ethoxide, sodium propoxide, and sodium butoxide. Reactions involving alkaline catalysis are about 4000 times faster than the reactions containing same amount of acid catalyst, and hence is more commercially viable. The

glycerides and alcohol used in alkaline catalysis must be anhydrous, as presence of water causes saponification, which is the process of formation of soap from fats. The soap reduces efficiency of the catalyst. Saponification also leads to gel formation that increases viscosity, inhibiting separation of products. Stoichiometry is an important consideration, as 3 mol of alcohol is required for 1 mol of triglyceride to produce 3 mols of FAME and 1 mol of glycerol. However, research has shown that most oils like peanut oil, soybean oil, sunflower oil and cotton seed have higher efficiency at 6:1 ratio of alcohol to oil (triglyceride) rather than 3:1, and hence that is what is used as an industrial standard. [4, 26, 28-29]

1.3.6.2.3 Enzyme Catalysis. The third method of catalysis is enzyme catalysis. In enzyme catalysis, the reaction proceeds in a way that produces FFAs. The triglycerides are first converted into FFAs by lipase enzymes and are subsequently converted into methyl esters by esterification with methanol. This alleviates issues with FFA content in used oils since the catalysis is done by an enzyme. By using lipases as catalysts, various types of alcohols, like primary, secondary, branched etc. can be used. Various researchers have determined that with primary alcohols the yield is about 94.8 - 98.5%, while secondary alcohols show a broader range of about 61.2 - 83.8%. The biggest disadvantage of using enzymes is the high cost of obtaining and processing them. [4, 26, 30-31]

1.4 Experimental Pyrolysis Result

As mentioned before, pyrolysis is an efficient process of making biodiesel a more usable source of automotive fuel. Pyrolysis of FAMEs is experimentally done in a stainless-steel tube with various inlets and outlets to let vapors and other byproducts leave. The process is done at a

variety of temperatures to probe the effect of temperature on the pyrolysis procedure and products.

The results of pyrolysis of methyl oleate has shown production of various smaller molecules. [4, 26, 28] Cis-trans isomerization and hydrogenation of double bonds are observed as the reaction proceeds. Formation of H_2, CO, CO_2, methane, n-paraffins, α-olefins, aromatics, smaller esters, and minor products including coke, diolefins etc is seen in these investigations. These molecules further undergo radical chain scission to form lower molecular weight FAMEs and 1-alkenes and alkanes.

Experimentally, the CO:CO_2 ratio changes to temperature fairly uniquely. It can be used to correlate the computational results to experimental temperatures. Experimentally, the ratio is seen to be around 0.01 - 0.4 with increasing ratio corresponding to increase in temperature. The amount of CO_2 produced experimentally generally remains similar throughout myriad temperatures, but the amount of CO increases with temperature (and hence the CO:CO_2 ratio increases). This ratio is important as it shows the extent of deoxygenation of the compound.

Pyrolysis is an experimentally tedious and expensive process. Trial and error regarding an optimum temperature and FAME selection can be costly both in terms of money and labor. Hence, in this investigation, we simulate the method computationally. This will help optimize the process temperature, the FAME structure and, based on products, can also help make changes to the process for more desirable product formation.

Experimentally, pyrolysis can be carried out on triglycerides directly. [32] However, modelling pyrolysis directly from the triglyceride presents several problems: 1) the computational cost for such simulations is intractable with the methods described herein (triglycerides, three-times as large as FAMEs, take ~250 times as long to simulate), 2) the

triglycerides' branched structures exhibit more weak intramolecular interactions that are poorly described by DFT. Since FAMEs essentially represent a substructure within a triglyceride, FAMEs are used as the starting material for pyrolysis.

CHAPTER 2: INTRODUCTION TO COMPUTATIONAL CHEMISTRY

2.1 Chemical dynamics simulation

2.1.1 Molecular Dynamics. Molecular dynamics (MD) simulations are computational method that models the movement of atoms and molecules. The particles interact for a fixed amount of time, and the dynamic evolution of the system can be determined by numerically solving Newton's equations of motion. The simulations require determination of the potential energy to determine the force experienced by an atom with respect to the positions of other atoms in the system. [47]

Newton's equations of motion play a very important role in MD simulations. The second law of motion relates force to mass and acceleration of a particle:

$$F=ma$$

where, F is the force experienced by the atom, m is the mass of the atom and a is the acceleration. As a function of the position, x, the force of an atom can be denoted as follows:

$$F(x) = - \nabla U(x)$$

where, x represents the coordinates of all atoms and U is the potential energy function. Using this equation, the potential energy with respect to position is calculated, and then the experienced force by each atom with respect to the positions of other atoms is determined.

The basic algorithm in an MD simulation requires numerical integration with respect to time where the infinitesimal time steps are normally a few femtoseconds (10^{-15} s). The forces acting on each atom are the then computed using a molecular mechanics force field (a force field in molecular modelling is the parameter sets used to calculate the potential energy of a system of

atoms). [48] The atoms are then moved a bit, and then their position and velocity are calculated using Newton's Law of motion, and the previous steps are repeated.

2.1.2 Temperature accelerated molecular dynamics. Conventional constant temperature methods used in molecular dynamics are commonly used to investigate various factors involving conformations and dynamics. The time steps of such processes are generally at the range of nanosecond to microseconds of experimental time. These larger time steps contribute to infrequent skips in different phases of the system, and hence the whole system might not be mapped out properly. [42] The reason for this might be large energy barriers between low energy points in the potential energy surface.

To solve the mentioned issues, TAMD is introduced. TAMD stands for temperature accelerated molecular dynamics and follows the system on the picosecond time scale, hence not skipping crucial information like interaction between C-H bond. It does so by 'flooding' the potential energy surface. Most of the times analyzing a single trajectory reveals various characteristics of the system. [43]

2.1.3 Atom-centered density matrix propagation. Atom centered density matrix propagation (ADMP) is a molecular dynamics model that belongs to the extended Lagrangian approach to molecular dynamics using Gaussian basis functions and propagating density matrices. The most common method of this type is Car-Parrinello (CP), where Kohn-Sham molecular orbitals are chosen as the dynamical variables to represent the electronic degrees of freedom. [49] CP calculations employ Kohn-Sham density functional theory (DFT) orbitals expanded in plane-wave basis sets.

ADMP has many advantages when compared to previous methods. ADMP uses atom-centered Gaussian basis sets. Hence, ADMP helps in prevention of poor energy conservation

during trajectory calculations, when used with Gaussian basis functions. ADMP provides some versatility of treating each electron in the system separately or using pseudopotentials to describe core potentials. ADMP also helps in better computation by using fewer basis functions per atom, while getting more time steps, being very accurate and more efficient. ADMP also allows one to visualize geometric and dynamic bond activity as time progresses during trajectory calculations. [49]

2.1.4 Stochasticity. Stochasticity is the quality of lacking any predictable order or plan (denotes randomness). Stochastic refers to a randomly determined process. In quantum mechanics, stochasticity through space and time is important. Spacetime stochasticity is the idea that small-scale structure of spacetime is undergoing both metric and topological fluctuations. These aberrations occur because of the presence of persistent vacuum fluctuation. [50]

Having a stochastic ensemble helps in predicting a range of possibilities as to the outcome of a trajectory, rather than having a single predictable outcome. [50] The multiple simulations help to account for various sources of uncertainties in the simulations namely velocity and heat transmissions through the bonds. Having a statistically valid ensemble of trajectories helps in forecasting the results to facilitate design of an optimum FAME.

For considering all the states present in the system, sufficient number of dissociated trajectories must be evaluated. This will be in conjunction with the ergodic hypothesis, which states that randomness repeated enough number of times will lead to obtaining most states present in the system. This leads to more accurate results and does not lose information.

2.1.5 Nuclear kinetic energy. For all forms of MD simulations, the kinetic energies of the nuclei need to be specified. The nuclear kinetic energy (NKE) helps for instant propagation of kinetic energy to facilitate random velocities of the nuclei. This is necessary as neither energy

nor velocity are conserved in these calculations. [44] The nuclear kinetic energy of the system is given by:

$$NKE = \frac{3}{2}(N-1)k_B T$$

where, N is the number of nuclei, k_B is Boltzmann Constant and T is the temperature of the system in K.

2.1.6 Disadvantages of molecular dynamics. Molecular dynamics simulations are an important step for simulating physical movement of atoms in a system, but it has disadvantages. One of the most important drawbacks is the time steps of the calculation, which is on the order of nanoseconds for large systems. Having a larger time step causes a loss of resolution in faster interatomic interactions like C-H bond vibrations (they would not be accurately observed). [52]

The nanosecond limit also restricts configurational sampling that can be achieved. A lot of various conformational changes, such as protein folding and faster bond interactions (vibrations), happens very fast (at fs order, and hence information, such as fast bond vibrations, are lost. This restricts the amount of thermodynamic information that involve entropy. [52]

Molecular dynamics also leads to increased computational cost. It is because of the quantum mechanical treatment of larger molecules for ab initio molecular dynamics that commands more computational prowess.

The final drawback is that the molecular dynamics simulations calculate electronic energy with respect to position of the atoms. This neglects the effect of entropy on the system that leads to loss of thermodynamic stability. [52]

2.2 Electronic structure theory

Electronic structure theory refers to the motion of electrons in atoms and molecules. [33] In quantum chemistry, electronic structure refers to the motion of electrons due to an electric field

that is created by a nucleus/arrangement of nuclei. This term covers both the wave function and related energies of the electrons. [33]

2.3 Born-Oppenheimer approximation

Electronic structure theory generally makes use of the Born-Oppenheimer (BO) approximation. The BO approximation is the assumption that the motion of an electron and a nucleus in an atom are decoupled, that is, can be treated separately during various calculations. [38] This approximation is made as nuclei are much heavier than electrons, and hence are slower to respond to external disturbances than electrons. Hence, given the same kinetic energy, the nuclei move much slower than electrons.

Mathematically, the BO approximation helps in expression of the wavefunction of a molecule as a product of the electronic wavefunction and the nuclear (vibrational, rotational) wavefunction:

$$\Psi_{total} = \psi_{electronic}.\psi_{nuclear} \qquad (2.1)$$

This decoupling makes electrostatic calculations mathematically tractable.

The BO Approximation is applied in two steps. In the first step, the nuclear kinetic energy is neglected, and hence, the T_n (nuclear kinetic energy) is removed from the total molecular Hamiltonian. [34, 35, 36]

The electronic Schrödinger equation is given by eq. 2.2.

$$H_e(e,R)\chi(r,R) = E_e\,\chi(r,R) \qquad (2.2)$$

The quantity r denotes electronic coordinates, R denotes nuclear coordinates and χ denotes the wavefunction. The eigenvalue for electronic energy (E_e) is dependent on various values of R.

Changing the values of R by a very small amount and calculating the energy gives E_e as a function of R determines the potential energy surface, $E_e(R)$. [36]

For the second step, the nuclear kinetic energy (T_n) is included, and the Schrödinger equation is given as:

$$[T_n + E_e(R)]\phi(R) = E\phi(R) \qquad (2.3)$$

This step includes separation of vibrational, translational and rotational motions. The eigenvalue E denotes the total energy of the molecule and includes effects from electrons, nuclear vibrations and overall rotational and translational motion of molecules. [34, 36, 37] BO approximation also facilitates the formation of a potential energy surface (PES). The potential energy surface denotes the energy of a molecule as a function of the position of atoms of the molecule.

2.4 Wave function theory

In quantum mechanics, a wave function is a mathematical description of the quantum state of an isolated quantum system. [34] Using wave functions, the probabilities of the possible results of measurements made in the system can be derived. The main factors that determine the wave function are degrees of freedom corresponding to the maximal state of commuting observables. [34-35] A commuting observable is a set of operators whose eigenvalue determines the state of the system.

In the previous section, we saw the electronic Schrödinger equation (2.2). This is derived from the time-independent Schrödinger equation after implementation of the BO approximation.

The expanded version of the equation is shown below:

$$[-\frac{1}{2}\sum_i \nabla_i^2 - \sum_{A,i}\frac{Z_A}{r_{Ai}} + \sum_{A>B}\frac{Z_A Z_B}{R_{AB}} + \sum_{i>j}\frac{1}{r_{ij}}]\boldsymbol{\Psi}(\boldsymbol{r};\boldsymbol{R}) = \boldsymbol{E_{el}}\boldsymbol{\Psi}(\boldsymbol{r};\boldsymbol{R}) \qquad (2.4)$$

where, ∇^2 is the Laplacian operator ($\frac{\partial}{\partial x^2} + \frac{\partial}{\partial y^2} + \frac{\partial}{\partial z^2}$), Z is the atomic number, r is the set of electronic coordinates and R is the set of nuclear coordinates.

2.4.1 Hartree-Fock theory. Hartree-Fock is a method of approximation to determine the wave function and the energy of a quantum many-body system at a stationary state. It is a common method used in computational chemistry and physics. [36]

Hartree-Fock Theory, also known as the Self Consistent Field (SCF) method, is the basis of molecular orbital theory, which says that individual electronic motion can be described by a single-particle function (orbital) and does not depend on the motion of other particles. [34-36] However, only one-electron systems such as hydrogen atom or He_2^+ have orbitals that are exact eigenfunctions of the full electronic Hamiltonian. [36]

The assumption of no interelectronic interaction is a significant approximation, and due to this, the total electronic wavefunction describing the motion of multiple electrons is a product of individual single electronic Hamiltonians:

$$\Psi_{HP}(r_1, r_2, r_3, \ldots, r_N) = \phi_1(r_1)\,\phi_2(r_2)\,\phi_3(r_3)\ldots\ldots\ldots\,\phi_N(r_N) \qquad (2.5)$$

Ψ_{HP} is called the Hartree Product, which determines the many-particle wavefunction of a system by combining the wavefunction of the individual particle wavefunctions.

This form of the equation has a major disadvantage; it does not satisfy the antisymmetry principle (Pauli exclusion). [4] To solve this problem, Hartree-Fock assumes that the exact *N*- body wave function of a system can be approximated by a single Slater Determinant, in case of fermions, of *N* spin orbitals. For spin orbitals, it is seen that fermions have an additional intrinsic spin coordinate, in addition to three spatial degrees of freedom. [35, 37] A set of spin coordinates can be represented as:

$$X= \{r, \omega\} \tag{2.6}$$

where ω is a generic spin coordinate.

Hence, the spatial orbital, ϕ(r) can be replaced by the spin-orbital, χ(x), where:

$$\boldsymbol{\chi_N(x_N)} = \phi(r)\alpha$$

where α is the spin function. This gives us the Hartree Product as:

$$\Psi_{HP}(x_1, x_2, x_3,.,x_N) = \chi_1(x_1)\,\chi_2(x_2)\,\chi_3(x_3)...\,\chi_N(x_N) \tag{2.7}$$

However, it is seen that even this change does not satisfy the antisymmetry principle. The reason can be seen when this equation is used for a 2-electron system:

$$\Psi_{HP}(x_1, x_2) = \chi_1(x_1)\,\chi_2(x_2) \tag{2.8}$$

If the coordinates of the two electrons are swapped, the wavefunction is given as:

$$\Psi_{HP}(x_1, x_2) = \chi_1(x_2)\,\chi_2(x_1) \tag{2.9}$$

For the antisymmetry principle to be satisfied, the exchanged coordinates must be the inverse of that for the original, as shown below:

$$\chi_1(x_1)\,\chi_2(x_2) = -\chi_1(x_2)\,\chi_2(x_1) \tag{2.10}$$

This is not going to be true in real situations, and hence, there is a need to find a solution to this.

2.4.1.1 Slater determinants. The Slater determinant is an expression used to describe the wavefunction of a multi-electron system that satisfies the antisymmetry principle. [34] The wavefunction using Slater determinants for a 2-electron system is given by:

$$\Psi_{HP}(x_1, x_2) = \frac{\mathbf{1}}{\sqrt{2}}[\chi_1(x_1)\,\chi_2(x_2) - \chi_1(x_2)\,\chi_2(x_1)] \tag{2.11}$$

This functional form can be put as:

$$\Psi_{HP}(x_1, x_2) = \frac{\mathbf{1}}{\sqrt{2}}\begin{vmatrix} \boldsymbol{\chi_1(x_1)} & \boldsymbol{\chi_2(x_1)} \\ \boldsymbol{\chi_1(x_2)} & \boldsymbol{\chi_2(x_2)} \end{vmatrix} \tag{2.12}$$

This form agrees with Pauli Exclusion Principle, as trying to put two electrons in the same orbital, gives the wavefunction to be 0. Therefore, for *N* particles, the slater determinant is given by:

$$\Psi = \frac{1}{\sqrt{N!}} \begin{vmatrix} \chi_1(x_1) & \chi_2(x_1) & \ldots & \chi_N(x_1) \\ \chi_1(x_2) & \chi_2(x_2) & \ldots & \chi_N(x_2) \\ \ldots & \ldots & \ldots & \ldots \\ \chi_1(x_N) & \chi_2(x_N) & \ldots & \chi_N(x_N) \end{vmatrix} \quad (2.13)$$

This notation shows that the electrons are indistinguishable, and each orbital is characteristic to each electron. Another issue is that swapping values in the determinants leads to inversion of signs, which brings about an issue regarding anti-symmetry.

2.4.1.2 Hartree- Fock- Roothaan equations. The Hartree- Fock theory, as mentioned before, is used to solve the electronic Schrödinger Equation, and it assumes that the wavefunction can be approximated by a Slater determinant made up of one-electron orbital. It helps in determining the minimum energy molecular orbitals for a system with given atomic orbital state. There are three approximations that are done to obtain the necessary equation. [34-37] The first one is the BO approximation, which states that the nuclei are stationary and that there is negligible interaction between nuclear and electronic motion. The second one is the mean field approximation, which states that there is no discrete interelectronic interactions, but the electrons interact with the mean field of the other electrons present in the system. The third one is the usage of a finite set of orbitals, which is a basis set, in which the spin orbitals can be expanded.

The Hartree-Fock-Roothaan equation is given by:

$$\sum_v F_{\mu v} C_{vi} = \epsilon_i \sum_v S_{\mu v} C_{vi} \quad (2.14)$$

where, ϵ is a diagonal matrix of the orbital energies ϵ_i, *C* are the coefficients of the eigenfunctions. $F_{\mu v}$ and $S_{\mu v}$ are matrix element notations, and can be expanded as:

(2.15)

$$F_{\mu\nu} = \int dx_1 \, \tilde{\chi}_\mu^*(x_1) \tilde{\chi}_\nu(x_1)$$

$$S_{\mu\nu} = \int dx_1 \, \tilde{\chi}_\mu^*(x_1) f(x_1) \tilde{\chi}_\nu(x_1) \quad (2.16)$$

where, $\tilde{\chi}$ is the orbital basis function denoted by:

$$\chi_i = \sum_{\mu=1}^{K} C_{\mu i} \tilde{\chi}_\mu$$

The Hartree-Fock-Roothaan equation is most simply denoted as

$$FC = SC\epsilon \quad (2.17)$$

where, F is the fock matrix (matrix approximating the single electron energy operator of a given quantum system in a given set of basis vectors), *S* is the overlap matrix (square matrix used to describe the inter-relationship of a set of basis vectors of a quantum system) of the basis functions and ϵ is a diagonal matrix of the orbital energies.

2.5 Density functional theory

As mentioned earlier, the quantum mechanical wavefunction signifies the information about a specific system. The solution to the Schrödinger equation gives the wavefunction of the system. However, to solve the Schrödinger equation for an N-electron system is almost impossible for N>1. Density Functional Theory is a quantum mechanical method to determine an definite solution to the Schrödinger equation of a many-body system.

Density Functional Theory investigates the ground state electronic and nuclear structures. The main entities studied are atoms, molecules and condensed phases. [39] Various properties of a many-body system can be obtained using a functional, which is a function of another function. As the name suggests, the functional here is that of electron density, which in turn is a function of space and time. This makes DFT more efficient when compared to older methods such as

Hartree- Fock that use electron correlation (using mean field of electrons rather than instantaneous electron-electron repulsion). It is because the electronic wavefunction is the function of the coordinates of all atoms in the molecules (3N for when the number of atoms are N and the three Cartesian coordinates, x, y and z). [34, 40] Hohenburg and Kohn brought electron density into the spotlight through their existing Hohenburg- Kohn theorems. The first theorem states that electronic density of any system can help determine all ground state properties of the system. [41] In this case the total ground state energy of a many-electron system is a functional of density, and hence, by solving the electron density functional, the total energy of the system can be determined.

2.6 Required input for computational calculations

There are various important factors that are needed to carry out a computational chemistry calculation. The first thing to consider is the type of calculation that is being carried out. Based on the type of calculation, the selection of an appropriate model chemistry (energy operator plus basis set) needs to be done. Then, more intricate details entailing the type of molecule is mentioned for proper electronic calculations.

There are three types of electronic structure calculations conducted in this investigation. The first is the determination of energy for a molecular geometry. The second is optimization of molecular geometry to a local minimum on the potential energy surface. The third is determination of the vibrational normal modes for a given local minimum. [34]

Electronic structure methods are utilized that use laws of quantum mechanics to compliment molecular dynamics. As mentioned before, the Schrödinger equation is used to determine the energy states and other related properties. Ab initio methods of quantum

computational methods use correct Hamiltonian, which involves the energy operators and help in consideration of different factors that help in accurate calculation of energy, and use just necessary experimental fundamental constants, in contrast to semi-empirical methods, that use a simpler Hamiltonian that is adjusted to fit experimental data. [46] In quantum mechanics, electron configurations of atoms are encompassed within the wavefunction. Computationally, the wave function is constructed from functions supplied to each atom through linear combination. This linear combination of atomic orbitals (LCAO) makes up the basis set, which helps in depicting the electronic structure more accurately. [40, 53]

Requirements involving the molecule require certain specific information. The first of them is the atomic coordinates. Atomic coordinates help to specifying three dimensional molecular structures. They are specified X, Y and Z Cartesian coordinates. [45-46] The next factor is the type of atoms present in the system under consideration. This is important as it helps denote the electronic features of various atoms for accurate electronic interactions during the calculation. Also, the types of atoms present designate the bonds which are not denoted by atomic coordinates. Specific atomic distances help in designating covalent bonds between atoms. [45-46]

Another important input is the charge and multiplicity of the molecule. Charge denotes if there is presence of an overall positive or negative charge in the molecule. Multiplicity depends on the total spin angular momentum (configuration using the determinant), also denoted by the total number of unpaired electrons plus one. These help in determination of the number of electrons and the electronic configuration of the molecule. [45-46]

CHAPTER 3: COMPUTATIONAL METHODS

3.1 Model Chemistry

For our choice of model chemistry, we draw heavily from Wilson et. al.[54], who report the performance of several quantum chemical methods to determine gas phase thermodynamic properties of FAMEs. Operators tested included B3LYP, B97-D, MP2 and M06-2X. Various basis sets were also tested, including 6-31G(d), 6-31+G(d,p), 6-311++G(2d,p), cc-pVDZ and aug-cc-pVDZ. Efficiency of the process was assessed using homolytic bond dissociation energies for various operators combined to different basis sets. Of all the model chemistries, M06-2X/6-31+G(d,p) had the lowest mean average percent deviation[54, 55]. Hence, M06-2X/6-31+G(d,p) was chosen as the model chemistry herein. M06-2X is a method developed by Truhlar and Zhao that was parameterized to describe the thermochemistry, kinetics and noncovalent interactions of main-block elements.M06-2X is able to describe π-π interactions, hydrogen bonding and long range forces. [59] These are important factors as the molecule in investigation, methyl oleate, has a π bond and due to presence of various atoms with varying electronegativity, hydrogen bonding is also an important consideration.

3.2 Temperature Studies

Various temperatures must be evaluated to determine the optimum dissociation temperature which is the lowest temperature that will reliably dissociate the molecule at the given timeframe of the FAME. If the temperature is too low, the bonds will not get enough energy to dissociate on the simulated time-scale. If the temperature is too high there will be unrealistic dissociation rates and products. Too high temperature also leads to deviation from

PES. The temperatures investigated are 3500 K, 3750 K and 4000 K. These temperatures were determined based on works of previous lab members. [54, 60] It is important to note that such high temperatures are chosen to accelerate the rate of chemical reaction to an extent that events observed on the simulated time scale correspond to the experimental time scale (much longer/lower temperature). Small microcanonical ensembles were initiated at each of the three temperatures starting at a single optimized structure of methyl oleate. At 3500 K, the dissociation percentage is 27%. At 3750 K, the dissociation percentage is 25% and at 4000K, the dissociation percentage is 83%. Therefore, 4000 K was chosen based on efficiency of dissociation and computational economy.

3.3 Dihedral Randomizer

Methyl oleate is a large, conformationally fluxional, molecule. Accurate depiction of its pyrolysis may depend on stochastic description of its conformation when exposed to heat. To address this, starting conformations are generated on-the-fly by varying dihedral angles within the molecule. A dihedral angle is defined by the angle between two planes. These two planes are defined by two sets of three atoms (two of which are common atoms). The rotatable C-C bonds in methyl oleate are shown in Figure 2 highlighted in green.

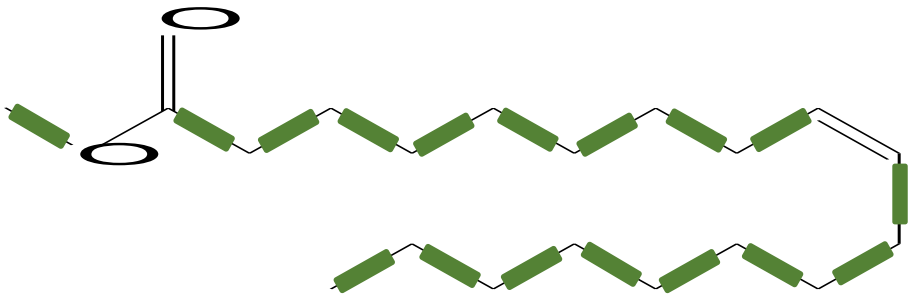

Figure 2. Rotatable dihedrals present in methyl oleate shown with green highlights.

These bonds are rotated by 60°, 180° or 300°, as these angles lead to a staggered conformation, which is relatively more stable. Changing the dihedral angles leads to an ensemble of conformers that may affect the location, frequency, and timing of bond breakage during pyrolysis. The randomization is achieved using an Excel program.

Some combinations of dihedral cause forbidden structures that involve overlapping atoms and bonds, so each combination generated above is visually inspected for validity before it is used in a simulation. If a combination is seen to be forbidden, it is discarded and then another randomization is taken for consideration.

CHAPTER 4: RESULTS AND DISCUSSION

A total of 75 dissociative trajectories were collected with pseudorandom starting conformation (of 75 trajectories initiated; 100% dissociation) Myriad products are observed from these trajectories. We first discuss ensemble statistical results, then trends by bond-type, followed by discussion of rare/unique products.

4.1 Ensemble Statistical Results

4.1.1 Homology plot. We aggregate the observed end products of the dissociations by the number of carbon atoms: so-called "homology." A substantial proportion of trajectories result in low molecular-weight (one- and two-carbon) products: 29.55% are one-carbon compounds including methyl free radical, formaldehyde and carbon monoxide; and about 31.06% are two-carbon compounds including ethane, ethene, etc. Homology plot for the investigation is shown in figure 3.

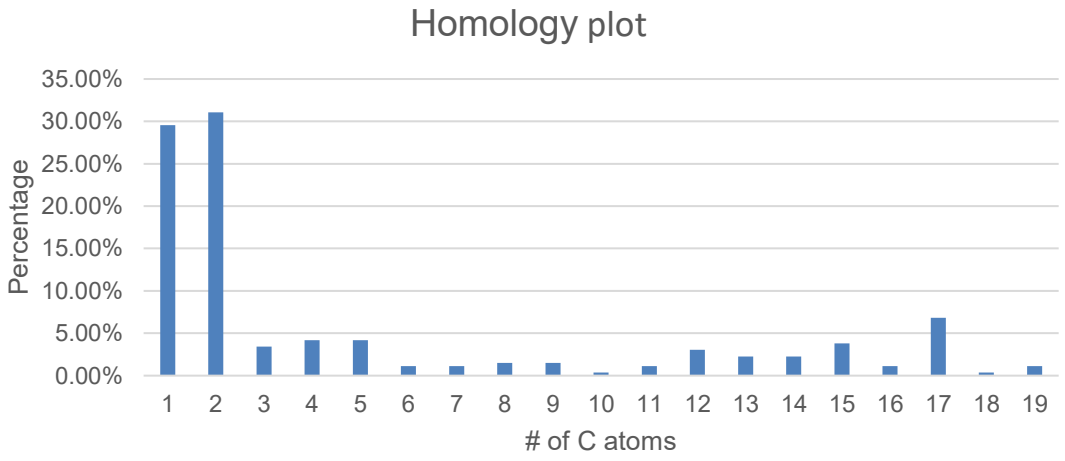

Figure 3. Homology plot: Frequency of observation for products based on the number of carbon atoms. We see that there are many 1 carbon and 2 carbon compounds and low frequency of 10 and 11 carbon compounds owing to the double bond present in the methyl oleate molecule.

A striking feature of Figure 3 is the substantial proportion of one- and two-carbon compounds. Products containing a single carbon atom are formed through dissociation of methyl carbon bonds and carbonyl carbon-oxygen bonds, which leads to methyl radical, methanol and/or formaldehyde (decarboxylation and deoxygenation). Note that many of the one-carbon compounds include oxygen, such as carbon monoxide, carbon dioxide, formaldehyde, etc.

The most abundant two-carbon product observed is ethene (~88% of products containing two carbons). Bakker described the proclivity for ethene formation as the zipper effect[60] It is a cascade of β-scission events that is illustrated in the Figure 4.

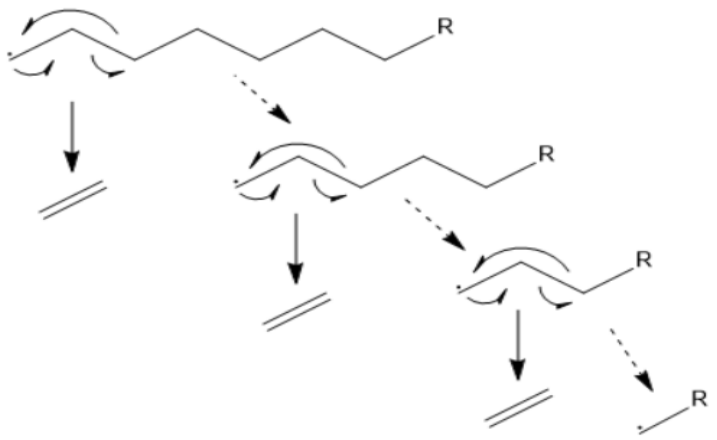

Figure 4. Illustration of zipper effect that shows formation of terminal free radical and facilitating β C-C bond scission, forming multiple ethenes and smaller hydrocarbon chains.

Aggregation of products observed in these simulation gives the pie chart in Figure 5. It is apparent that ethene is the most common product, followed by monounsaturated free radicals, and carbon monoxide. Other products include methyl free radical, saturated free radicals and formaldehyde. Other products seen in the investigation are carbon dioxide, hydrogen molecules, cyclic compounds and smaller methyl esters and methyl ester free radicals. All products of dissociation are shown in Appendix A.

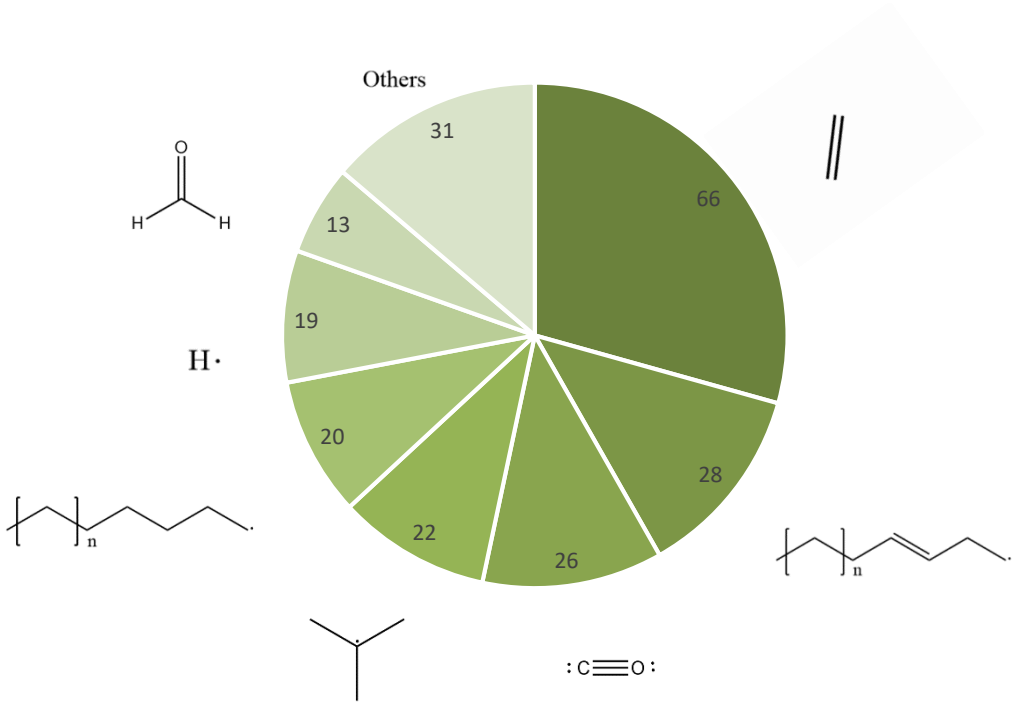

Figure 5. Distribution of major products observed in simulations described herein.

4.1.2. Time analysis. Table 2 compiles bond distances for those types of bonds found in methyl oleate, compute using covalent radii.

Table 2. Standard bond lengths of concerned bonds determined using covalent radii. [61]

Bond	Length(pm)
C-C	154
C-O	143
C-H	109
C=C	146
C=O	139
O-H	97

Bonds are considered broken when vibrational energy of the atoms exceeds the attraction forces between the species.

To quantify the time at which significant bond-breaking/-forming events take place covalent bond radii were used to create threshold interatomic distances. Proceeding to large distances beyond this threshold with persistence over time indicates a bond-breaking event (while the inverse represents a bond-forming event). The average bond lengths utilized herein are given in Table 2.

The times are classified into 2 parts: primary and cumulative. Primary dissociation times correspond to the time at which first dissociation of the parent molecule of each trajectory occurs. Cumulative dissociation times correspond to all the times at which dissociation occurs in each time interval in any molecule present in the trajectories. Frequency of dissociation at various time intervals is illustrated in Figure 6.

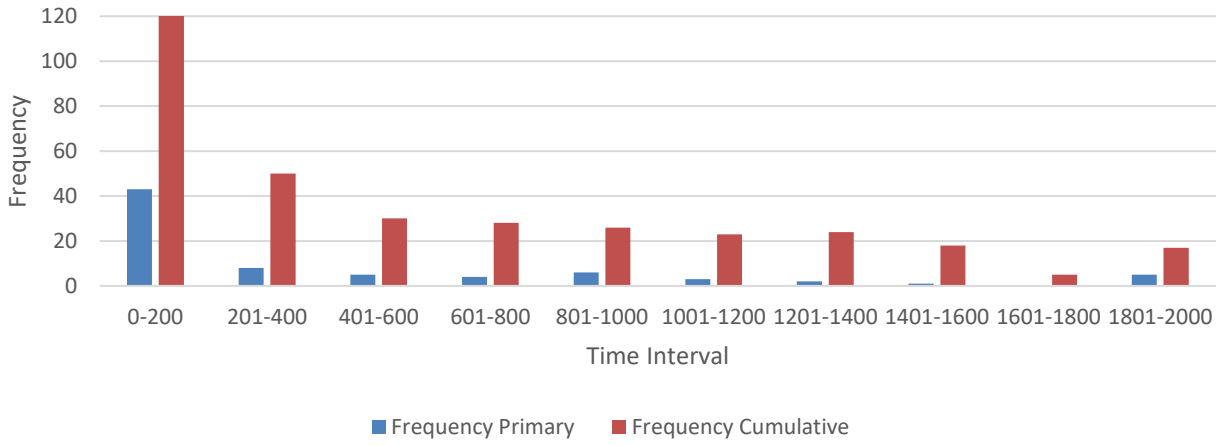

Figure 6. Frequency of dissociation at various time intervals showing two different classifications: First (Blue) indicating the first dissociations and Cumulative (Red) indicating an aggregation of all dissociations

Based on the plot, it is seen that there is a high frequency of dissociations in the first 200 fs. Most of the trajectories showed dissociations at less than 200 fs, but as steps progressed the dissociation frequency seems to decrease. The reason for this might be the fact that during such calculations the molecule folds before dissociating and hence the dissociation happens at a later stage. But in some of the random geometries, the molecule is already folded and hence the dissociation occurs at an earlier time. There are a few dissociations that are seen at the later part of the trajectories, but most dissociations are generally seen in the first 1400 fs. The next 600 fs does not see frequent dissociations.

4.2 Trends by Bond-Type

In this section we organize the data by bond-type in order of decreasing frequency of occurrence: C–C, C–H, then C–O bond dissociations, before going on to discuss bond-formations observed. The C and O atoms are numbered as illustrated in Figure 7.

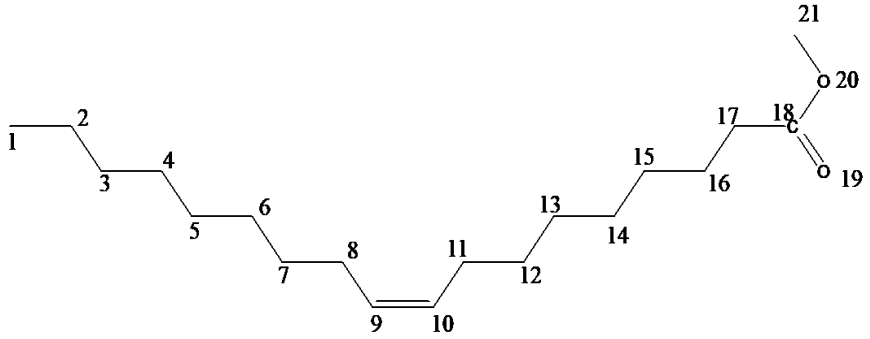

Figure 7. Structure of methyl oleate with atom numbers displayed using the Ω numbering system.

4.2.1 C–C bond dissociation. The ensemble results indicate that C–C bond breakage is the most commonly broken bond type. Of the 283 bond dissociations observed, 161 (56.89%) break a C–C bond. Since C–C bonds are the weakest bonds within methyl oleate [55] and bond homolysis is conventionally thought to occur selectively at the weakest bonding sites, this

observation makes sense. The frequency of bond dissociation along with each BDEs are shown in Figure 8.

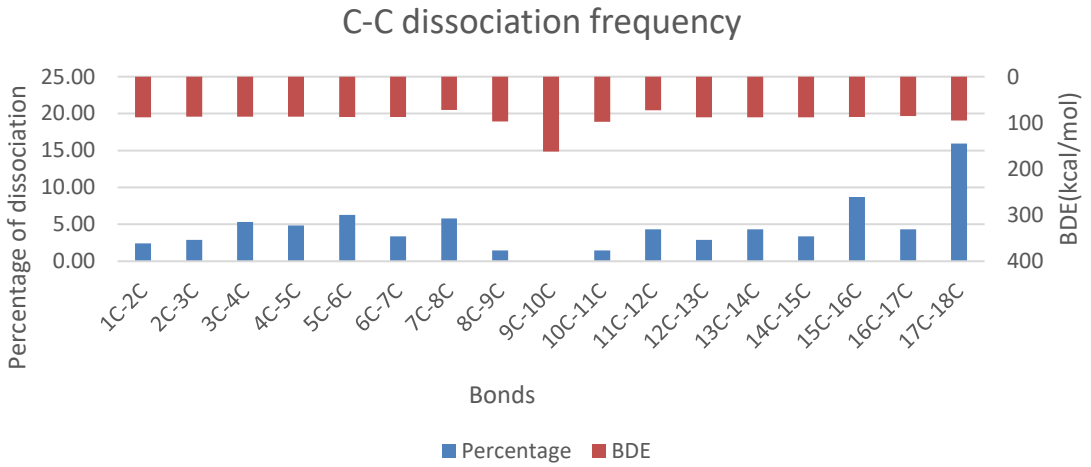

Figure 8. Plot between bond dissociation frequency (blue-bottom) and corresponding bond dissociation energies(red-top).

Of all C-C bond dissociations, we find that the C_{ipso}-C_{α} bond with respect to the carbonyl, 17C–18C bond breaks most frequently. The most common mechanism of these dissociations is α free-radical deoxygenation. The mechanism is shown in Figure 9:

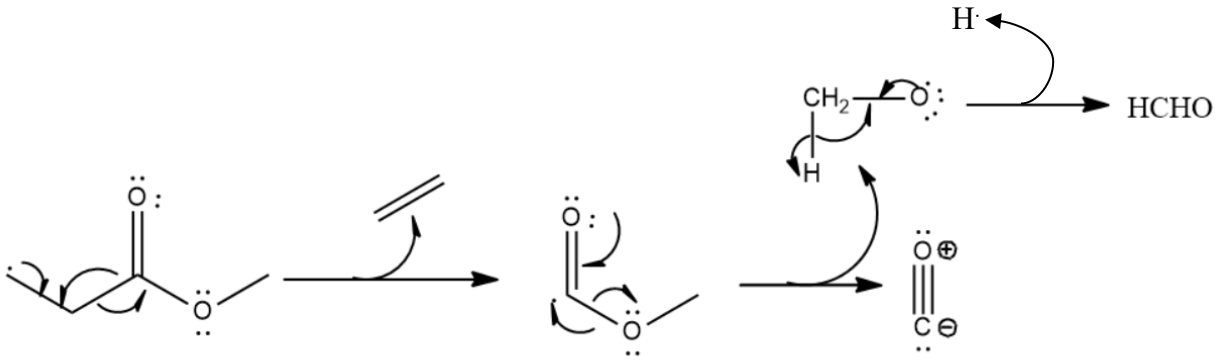

Figure 9. α free-radical deoxygenation process shows the dissociation of α-bond from the carbonyl bond.

Some of the bonds with the highest BDEs in methyl oleate include the two double bonds, 9C-10C and 18C-19O, and the bonds adjacent to the C-C double bond, 8C-9C and 10C-11C. Further correlation of observed dissociations and BDEs, we see that 9C-10C does not have any dissociation. It is evident from the fact that 9C-10C is a double bond with high BDE, making the π-bond along with the σ-bond much more difficult to dissociate than just a σ-bond. BDE of 8C-9C and 10C-11C are higher than the rest and is not seen to dissociate very frequently owing to the instability of the product of the dissociation. The allylic bonds within methyl oleate (7C-8C and 11C-12C) have lower BDE owing to resonance stability in the radical intermediates formed from dissociation, which facilitates their dissociations.

For 1C-7C and 12C-17C, we see the BDE is similar, but the dissociation frequency of these bonds varies a lot. This might be attributed to the zipper effect (Figure 4), where there are successive dissociations forming ethenes and smaller alkyl chains. Other methods for dissociations of C-H bonds are illustrated in Figure 10.

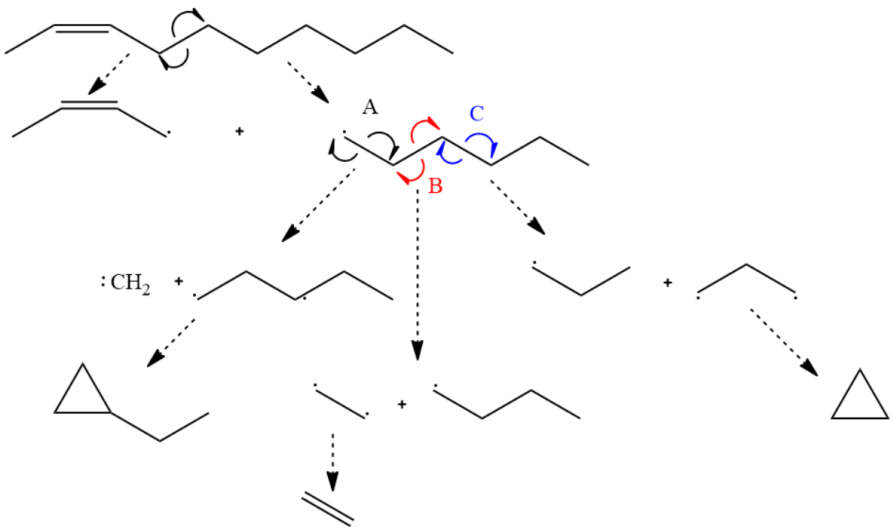

Figure 10. Mechanisms of different dissociations of C-H bonds illustrating different routes that can occur (A-black, B-red and C-blue), resulting in the formation of ethene, small alkyl chains and cyclopropyl derivatives.

4.2.2 C–H bond breakage. The trajectory analysis finds that C–H bonds are the second-most frequently cleaved bond type. Of the total 283 bond dissociations, 76 (26.86%) were C–H bonds. Figure 11 illustrates the frequency of C–H bond breakages.

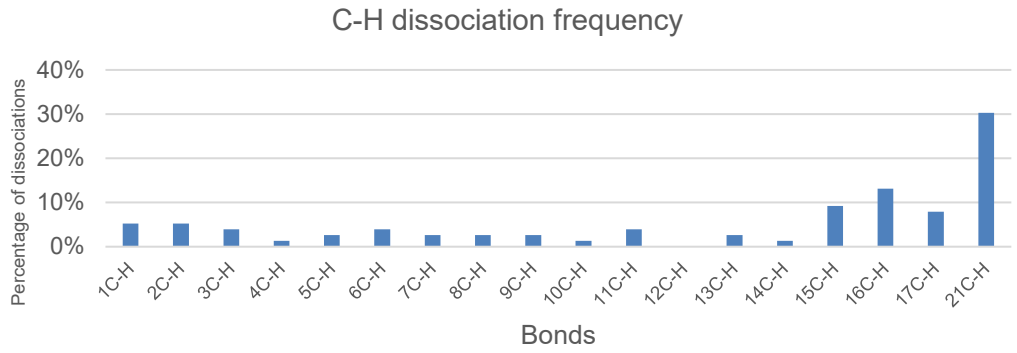

Figure 11. Percentage C-H bond dissociations corresponding to specific bonds dissociated.

Of note from Figure 11, is the large proportion of 21C-H dissociation observed. Dissociation of this bond leads to carbene and formaldehyde. The schematic is shown in Figure 12.

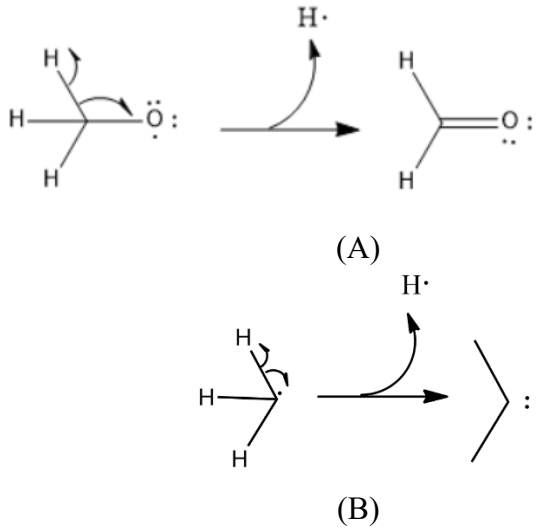

Figure 12. H-atom abstraction causing the formation of (A) Formaldehyde and (B) Carbene

Apart from the 21C-H dissociation, another frequent dissociation was 16C-H. This dissociation might be interpreted as a H-transfer to 17C, as 17C-18C is one of the most common bond dissociations that occur. The reason for the shift might be the increased stability of 2° free radical than 1° free radical. The mechanism for the same is illustrated in Figure 13.

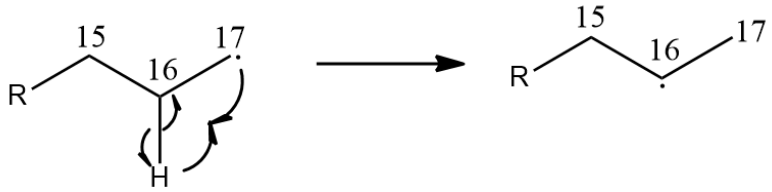

Figure 13. Formation of 2° free radical by hydrogen radical transfer causing an increase in stability from a 1° free radical.

Another result that comes from C-H bond dissociation is multiple H abstraction and reforming causing the formation of hydrogen molecule.

4.2.3. C–O bond breakages. The remaining type of bond breakage observed is the C–O bond breakages, constituting about 16.25% of the total dissociations. There are three C–O bonds in methyl oleate: 18C=O, 18C–O and 21C–O. We do not see any 18C=O bond cleavage considering the large bond-dissociation energy that comes with breaking σ and π bonds (here 169.7 kcal/mol). The C-O bonds generally dissociate with removal of CO (decarbonylation), removal of carboxyl group forming CO_2(decarboxylation) or removal of O atom causing the formation of aliphatic hydrocarbons(deoxygenation). Figure 14 illustrates the various methods of C-O bond dissociations.

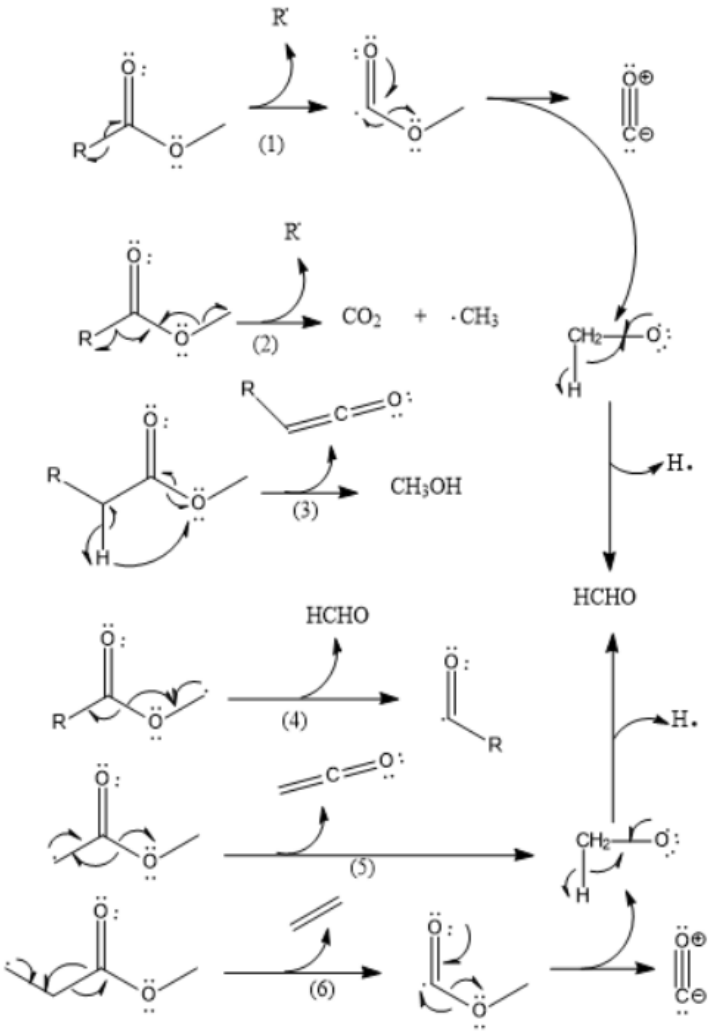

Figure 14. Various pathways for thermal decomposition. (1) Decarbonylation.(2) Decarboxylation. (3) Pericyclic deoxygenation. (4) Methyl free radical deoxygenation. (5) α Free Radical deoxygenation. (6) β Free Radical deoxygenation

4.2.4. Bond formations. Of the 75 trajectories currently analyzed, 52 show bond forming events. Bond formation has occurred in three ways during these pyrolysis simulations: 1) Hydrogen migration, 2) Cyclization, and 3) Rearrangement.

4.2.4.1. Hydrogen migration. This is the most commonly observed bond-forming event constituting 24.56%. Four different shifts are observed: 1,2-(Figure 15), 1,4-(Figure 16), 1,5-(Figure 17), and 1,11-(Figure 18) migrations.

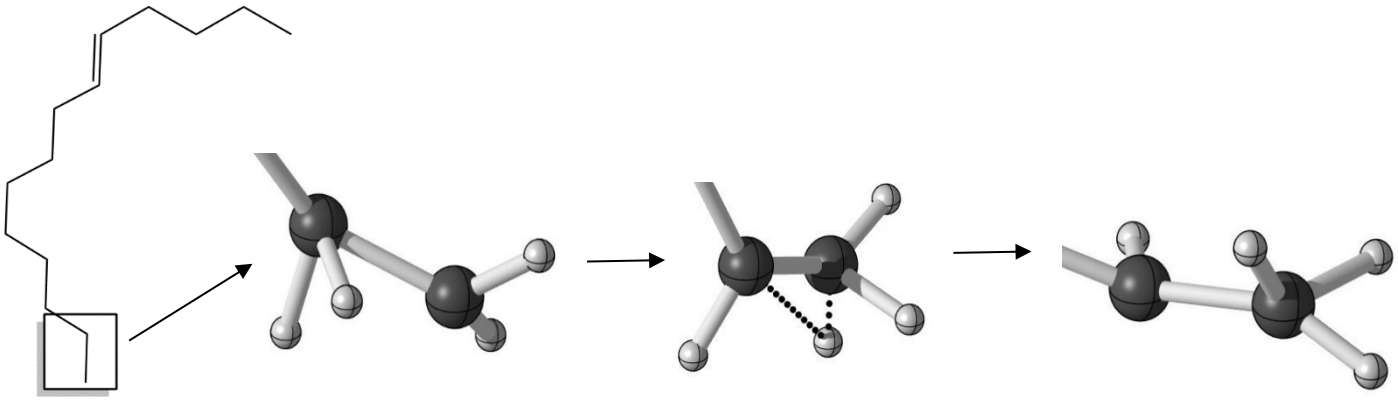

Figure 15. Representation of H-migration showing 1,2-Shift.

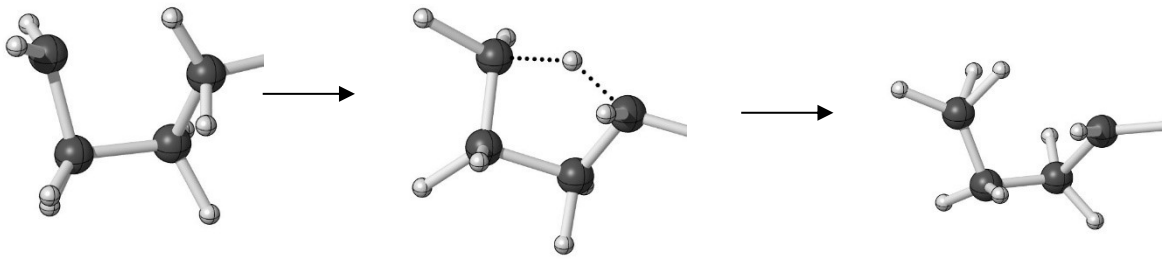

Figure 16. Representation of H-migration showing 1,4-Shift.

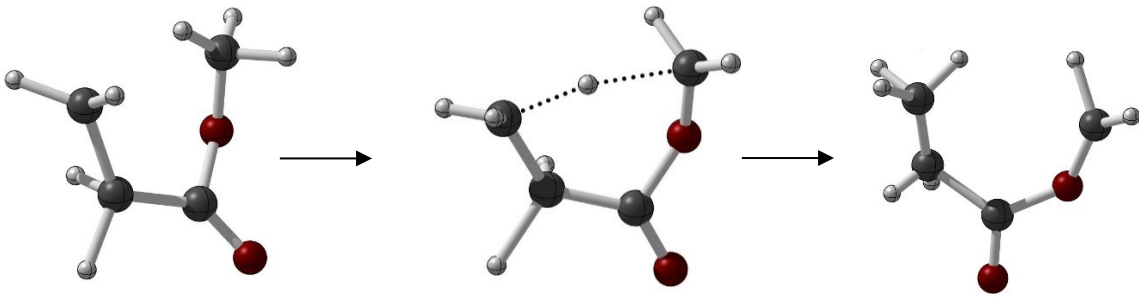

Figure 17. Representation of H-migration showing 1,5-Shift.

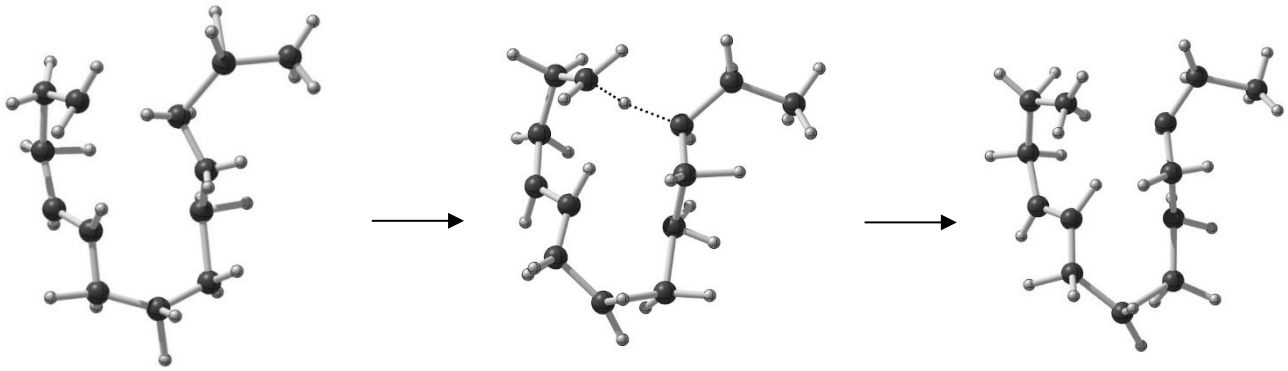

Figure 18. Representation of H-migration showing 1,11-Shift.

H migrations are generally observed for the purpose of increasing stability by the formation of a 2° radical from a 1° radical (Figure 10) or formation of a stable compound from a free radical. This occurs in 1,2-shift, 1,4-shift and 1,11-shift. This leads to an increased stability in the free radical compound.

The 1,5-shift causes a more stable radical by the formation of a free radical adjacent to a lone pair (e.g. beside an O atom). This stability in enhanced by the fact that the electron density from the lone pair on oxygen can be used to partially fill the orbital of the free radical carbon.

4.2.4.2. Cyclization. Now we look at the second type of bond formation. This sort of mechanism results in formation of cyclic compounds. There are 6 instances of cyclization that have been observed. These cyclizations lead to formation of cyclic compounds that mainly include cyclopropyl derivatives and one cyclohexyl compound. The mechanisms are illustrated in Figure 19.

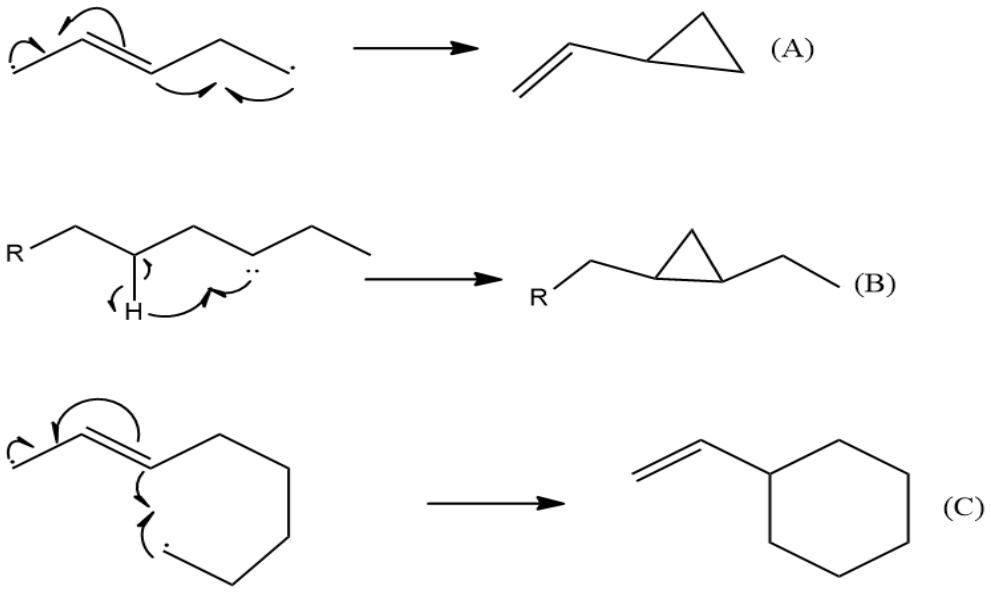

Figure 19. Methods of cyclization resulting in formation of vinyl cyclopropane derivatives(A), internal cyclopropane derivatives (B) and cyclohexane derivatves(C)

4.2.4.3 Rearrangements. In this sort of mechanism, the bond formation occurs between two atoms of different unbonded segments. It is a bond formation that follows a dissociation that occurs beforehand. Illustration of the same is shown in Figure 20.

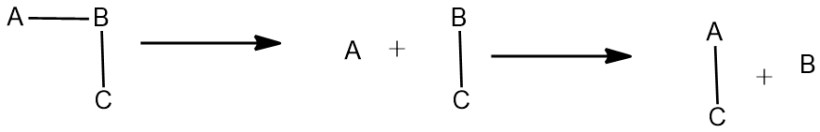

Figure 20. Illustration of rearrangement, where we see the transfer of an atom occurs between two atoms that dissociated previously.

This sort of formations generally occurs when two radicals come in proximity of each other and form a bond to produce a stable compound. The results of such formation lead to

formation of compounds such as methanol and ethane. Figure 21 illustrates the mechanism of the above-mentioned reactions.

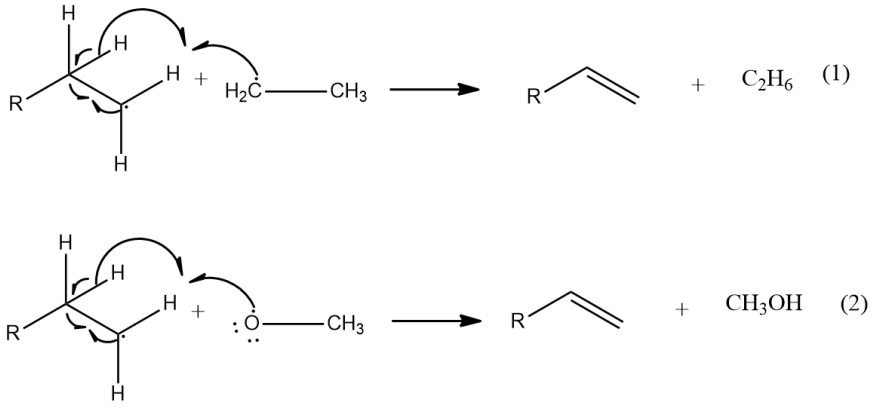

Figure 21. Rearrangement demonstrated where the H radical is transferred from the alkyl chain to the ethyl free radical (1) or the methoxy free radical(2).

The other type of molecule that can be generated from such a mechanism is methoxy methyl radical. It involves decarbonylaion reaction that involves formation of a reformation post dissociation of the atoms. The mechanism is illustrated in Figure 22.

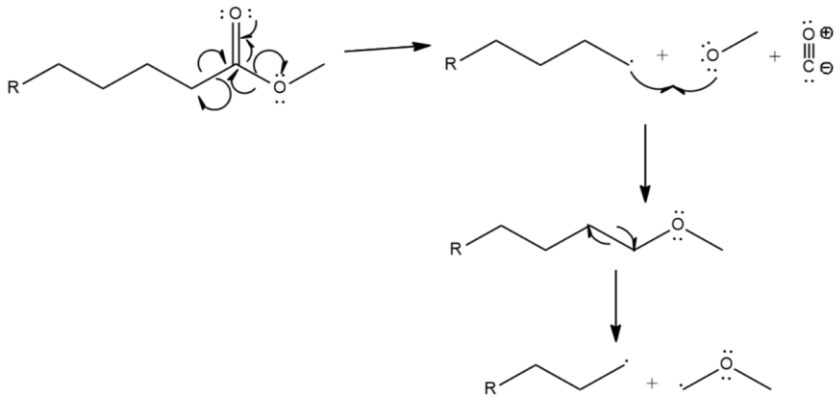

Figure 22. Decarbonylation reaction causing the formation of methoxy methyl free radical after reformation post dissociation.

4.3 Unique products

Experimentally, individual products of the analysis are left unidentified. Theoretical methods can be used to identify and categorize these products for better understanding of the process. Common unique products seen in this investigation are carbene (Figure 12), internal cyclopropyl derivatives (Figure 19(B)) and methoxy methyl radical (Figure 22). Analysis of these products give us a better view on the mechanism of pyrolysis that occurs and distribution of products. These products are used in certain other industries. For example, cyclopropane finds usage in pharmacological industry as an anesthetic and hence looking into the formation of cyclopropane can help in expanding this research into other industries.

4.4 Thermodynamic Analysis

Thermodynamically, a reaction is feasible if the change in Gibb's free energy of the forward reaction is negative. The change in Gibb's free energy is given as follows:

$$\Delta G_{reaction} = \Sigma G_{products} - \Sigma G_{reactants}$$

Feasible reactions where $\Delta G_{reaction}$ is negative are called spontaneous reactions and the ones that are positive are called non-spontaneous reactions. We have tried to determine the spontaneity of each of the trajectory by calculating the respective energies for each of the products and comparing it to that of methyl oleate.

The energy of each trajectory was calculated by determining the enthalpy, entropy and Gibb's free energy at 4000K of each of the products that are formed and adding them to form the enthalpy of products and Gibb's free energy of products. The energy of methyl oleate was calculated using an optimized structure. The change in Gibb's free energy, enthalpy and entropy

of the reaction are then calculated by subtracting the energies of the products from that of methyl oleate.

Of the 75 calculated trajectories, all of them are spontaneous. This agrees to the fact that a lot of energy was applied to the system as the calculations were done at 4000 K. Endothermic reactions are generally non-spontaneous. Due to the addition of high temperature, these reactions have become entropy driven. Gibbs' free energy expression based on enthalpy and entropy is given by

$$\Delta G = \Delta H - T\Delta S$$

where, ΔH is the change in enthalpy, ΔS is change in entropy and T is temperature in Kelvin. When the temperature of the system is very high (4,000 K for this investigation), the change in Gibbs' Free Energy is determined by the $T\Delta S$ factor, making entropy the driving factor for the spontaneity of the reaction. As is seen in appendix B, the entropy of all the trajectories are positive. The entropy also contributes to the fact that there are free radicals populating the dissociated trajectories which would rearrange and reform under normal circumstances. All the energies of the trajectories are given in Appendix B.

Now, we look at the trajectories with extraordinary change in Gibb's free energies. Some of the trajectories have higher negative Gibb's free energy (>-100 kJ/mol). These are less spontaneous than others. Most of these trajectories have products such as mono free radicals, carbene, methyl ester free radicals and a ketone in one instance. The other exceptional trajectories are the ones with high negative Gibb's free energy (<-500 kJ/mol). These trajectories are relatively more spontaneous. These trajectories generally dissociate into products such as ethene, larger alkenes, smaller methyl esters and carbon monoxide. These molecules are higher in stability and owing to their ease of formation and enhancing spontaneity.

There are certain products that are seen commonly in the dissociations that are highly spontaneous. These products have a higher probability of formation when such an investigation is carried out again. The most common products in these trajectories were ethene, cyclopropyl derivatives, carbon monoxide, 1-4 C alkyl free radicals and H free radical. Other products seen that are not common in all the highly spontaneous trajectories, but occur infrequently are buta-1,3-diene, hydrogen molecule, formaldehyde and larger alkyl free radical.

Change in Gibbs' Free Energy at 400 °C (673K) was also calculated using the change in enthalpy and entropy of each trajectory. Here we saw that most of the trajectories at 400K had positive ΔG value making the reactions non-spontaneous. The reason for this might be the endothermic nature of the reaction. This also explains the presence of free radicals and spontaneity of all the trajectories at 4000K, as it is a very high temperature and makes the reaction entropy dependent.

CHAPTER 5: CONCLUSION AND FUTURE WORK

M06-2X/6-31+G(d,p) was used to simulate thermal cracking of methyl oleate. TAMD at 4000 K was employed to simulate bond dissociation under application of heat. Each of the starting points of the trajectories were randomized using a program in Excel that facilitates suitable change in dihedral bonds, which leads to a more ergodic ensemble.

The most common product of dissociation observed is ethene, followed by monounsaturated free radical chains and carbon monoxide. Various products are left unidentified in certain experimental results and these are observed in theoretical ensemble. Analysis of these products gives more insight into mechanism of pyrolysis and might be able to provide more insight into expanding to other industries.

Experimental investigations show formation of CO, CO_2 1-4 C hydrocarbons, methanol, formaldehyde, smaller methyl esters, ketones, cyclopropane, carbonyl acids and 8-16C hydrocarbons, which are also seen in theoretical investigations. Products not seen in theoretical investigation but seen in experimental investigation are larger aldehydes and oxo-methyl esters.

However, the CO:CO_2 ratio determined by simulations was determined to be 2.6 whereas experimentally this ratio has been found to be between 0.01 to 0.4 at various based on different temperatures. [62, 63] The higher CO:CO_2 ratio and 100% dissociation of the calculated trajectories can be interpreted as the temperature of 4000 K to be too high.

The change in enthalpy and Gibbs' free energy was calculated for each of the dissociated trajectories. All the 75 trajectories are seen to be spontaneous. This agrees to the fact that large amount energy was supplied to the system at 4000K, which facilitates the reaction to be favourable.

The validity of this method has not entirely been established considering the effects of the high temperatures. A similar method at 3500K and without random starting points was performed by Michael Bakker [60] on methyl linoleate and promising results were found. His work had ~34% dissociations in terms of all the trajectories that were calculated, unlike this investigation which has 100% dissociations of all the trajectories. In a previous section we investigated the reason for using 4000 K, which was because of its higher rate of dissociation. But, the higher rate of dissociation might be due to too high of a temperature, which also facilitates formation of unstable products. This is also complimented by the fact that at 400 °C we see most of the reactions would be non-spontaneous.

Hence, the method used in this investigation needs to be optimized for more validation and proper temperature studies. The way to optimize this might be doing an investigation with the randomization of dihedrals using lower temperatures and see the difference in the dissociation rates. Another way might be to progressively decrease the temperature towards the end of the trajectory for equilibration. After the optimization, this method can be used to simulate pyrolysis on other fatty acid methyl esters such as methyl stearate, methyl linolenate etc. Following this, the ideal FAME for optimum pyrolysis in industry can be constructed by engineering it using the specific bonds that dissociate at optimum time and position.

REFERENCES

(1) Pogaku, R.; Raman, J. K.; Ravikumar, G. Evaluation of Activation Energy and Thermodynamic Properties of Enzyme-Catalysed Transesterification Reactions. *Advances in Chemical Engineering and Science* **2012**, 02 (01), 150–154.

(2) U.S. Energy Information Administration - EIA - Independent Statistics and Analysis https://www.eia.gov/.

(3) "EIA Energy Kids – Oil (petroleum)". www.eia.gov.

(4) Fukuda, H.; Kondo, A.; Noda, H. Biodiesel fuel production by transesterification of oils. *Journal of Bioscience and Bioengineering* **2001**, 92 (5), 405–416.

(5) Sheehan, J.; Camobreco, V.; Duffield, J.; Graboski, M.; Shapouri, H., An Overview of Biodiesel and Petroleum Diesel Life Cycles. *Agriculture, U. S. D*. o.; Energy, U. S. D. o., Eds. Golden, CO, **1998**; p 60.

(6) Multiphase Flow Model for Well Drilling. *Multiphase Flow in Oil and Gas Well Drilling* 2016, 75–96.

(7) Myers, D. R. Solar Radiation solar radiation for Solar Energy Utilization solar radiation for solar energy utilization. *Solar Energy* **2013**, 584–607.

(8) "2014 Key World Energy Statistics" iea.org. IEA. 2014. pp. 6, 24, 28.

(9) "Energy and the challenge of sustainability". United Nations Development Programme and World Energy Council. September 2000.

(10) Evans, A.; Strezov, V.; Evans, T. J. Assessment of sustainability indicators for renewable energy technologies. *Renewable and Sustainable Energy Reviews* **2009**, *13* (5), 1082–1088.

(11) "Global Installed Capacity in 2018". GWEC.

(12) Rinkesh. 7 Pros and Cons of Wind Energy http://www.conserve-energy-future.com/pros-and-cons-of-wind-energy.php.

(13) "History of Hydropower | Department of Energy". Energy.gov.

(14) Ingram, E.; Runyon, J.; Garvey, S.; Anton, L.; Maski, S.; Temeng, Y. T.; Lynch, D.; Hanawalt, S.; Corné, J.; Rudden, M.; et al. Hydropower https://www.renewableenergyworld.com/hydropower.

(15) Espa, P.; Batalla, R. J.; Brignoli, M. L.; Crosa, G.; Gentili, G.; Quadroni, S. Tackling reservoir siltation by controlled sediment flushing: Impact on downstream fauna and related management issues. *Plos One* **2019**, *14* (6).

(16) Markandya, A.; Wilkinson, P. (2007). "Electricity generation and health". Lancet. 370 (9591): 979–990. doi:10.1016/S0140-6736(07)61253-7. PMID 17876910

(17) Nuclear Power is the Most Reliable Energy Source and It's Not Even Close https://www.energy.gov/ne/articles/nuclear-power-most-reliable-energy-source-and-its-not-even-close.

(18) S., D. D.; M., D. M., Biodiesel Production From Animal Fats And Its Impact On The Diesel Engine With Ethanol-Diesel Blends: A Review. *International Journal of Emerging Technology and Advanced Engineering* **2012**, 2 (10), 179

(19) Iea. Transport biofuels – Tracking Transport – Analysis https://www.iea.org/tcep/transport/biofuels.

(20) Luo, Y.; Ahmed, I.; Kubátová, A.; Šťávová, J.; Aulich, T.; Sadrameli, S.; Seames, W. The thermal cracking of soybean/canola oils and their methyl esters. *Fuel Processing Technology* **2010**, *91* (6), 613–617.

(21) Knothe, G. “Designer” Biodiesel: Optimizing Fatty Ester Composition to Improve Fuel Properties†. *Energy & Fuels* **2008**, *22* (2), 1358–1364.

(22) Luo, Y.; Ahmed, I.; Kubátová, A.; Šťávová, J.; Aulich, T.; Sadrameli, S.; Seames, W. The thermal cracking of soybean/canola oils and their methyl esters. *Fuel Processing Technology* **2010**, *91* (6), 613–617.

(23) Zhang, Y.; Wang, X.; Li, Q.; Yang, R.; Li, C. A ReaxFF Molecular Dynamics Study of the Pyrolysis Mechanism of Oleic-type Triglycerides. *Energy & Fuels* **2015**, *29* (8), 5056–5068.

(24) Li, X.; Xu, X.; You, X.; Truhlar, D. G. Benchmark Calculations for Bond Dissociation Enthalpies of Unsaturated Methyl Esters and the Bond Dissociation Enthalpies of Methyl Linolenate. *The Journal of Physical Chemistry A* **2016**, *120* (23), 4025–4036.

(25) Sawangkeaw, R.; Bunyakiat, K.; Ngamprasertsith, S. A review of laboratory-scale research on lipid conversion to biodiesel with supercritical methanol (2001–2009). *The Journal of Supercritical Fluids* **2010**, *55* (1), 1–13.

(26) Moser, B. R. Influence of Blending Canola, Palm, Soybean, and Sunflower Oil Methyl Esters on Fuel Properties of Biodiesel†. *Energy & Fuels* **2008**, *22* (6), 4301–4306.

(27) Culhane, C. T. Functional Foods–New Perspectives. *Journal of Nutraceuticals, Functional & Medical Foods* **2003**, *4* (1), 67–77.

(28) Quesada-Medina, J.; Olivares-Carrillo, P. Evidence of thermal decomposition of fatty acid methyl esters during the synthesis of biodiesel with supercritical methanol. *The Journal of Supercritical Fluids* **2011**, *56* (1), 56–63.

(29) Diasakou, M.; Louloudi, A.; Papayannakos, N. Kinetics of the non-catalytic transesterification of soybean oil. *Fuel* **1998**, *77* (12), 1297–1302.

(30) Abigor, R. D.; Uadia, P. O.; Foglia, T. A.; Haas, M. J.; Jones, K. C.; Okpefa, E.; Obibuzor, J. U.; Bafor, M. E. Lipase-catalysed production of biodiesel fuel from some Nigerian lauric oils. *Biochemical Society Transactions* **2000**, *28* (6), 979–981.

(31) Ban, K.; Hama, S.; Nishizuka, K.; Kaieda, M.; Matsumoto, T.; Kondo, A.; Noda, H.; Fukuda, H. Repeated use of whole-cell biocatalysts immobilized within biomass support particles for biodiesel fuel production. *Journal of Molecular Catalysis B: Enzymatic* **2002**, *17* (3-5), 157–165.

(32) Fréty, R.; Maria Da Graça C. Da Rocha; Brandão, S. T.; Pontes, L. A. M.; Padilha, J. F.; Borges, L. E. P.; Gonzalez, W. A. Cracking and hydrocracking of triglycerides for renewable liquid fuels: alternative processes to transesterification. *Journal of the Brazilian Chemical Society* **2011**, *22* (7), 1206–1220.

(33) Simons, J. *An introduction to theoretical chemistry*; World Publishing Corp: Beijing, 2004.

(34) Cramer, C. J. *Essentials of computational chemistry: theories and models*; John Wiley & Sons: Chichester, 2017.

(35) Schreiner, P. R. *Computational molecular science*; Wiley-Blackwell: Chichester, 2014.

(36) Rinke, Patrick. *Electronic Structure Theory*. 11 Feb. 2014, http://www.fhi-berlin.mpg.de/~rinke/lecture.pdf

(37) Bauer, D. *Computational Strong-Field Quantum Dynamics Intense Light-Matter Interactions*; De Gruyter: Berlin, 2017.

(38) Cormen, Thomas H.., et al. *Introduction to Algorithms*. 3rd ed., MIT Press, 2009.

(39) http://newton.ex.ac.uk/research/qsystems/people/coomer/dft_intro.html.

(40) Koch, W.; Holthausen, M. C. *A chemists guide to density functional theory*; Wiley-VCH: Weinheim, 2010.

(41) Grimme, S. Semiempirical hybrid density functional with perturbative second-order correlation. *The Journal of Chemical Physics* **2006**, *124* (3), 034108.

(42) Abrams, C.; Bussi, G. Enhanced Sampling in Molecular Dynamics Using Metadynamics, Replica-Exchange, and Temperature-Acceleration. *Entropy* **2013**, *16* (1), 163–199.

(43) So/rensen, M. R.; Voter, A. F. Temperature-accelerated dynamics for simulation of infrequent events. *The Journal of Chemical Physics* **2000**, *112* (21), 9599–9606.

(44) Vimal, D.; Pacheco, A. B.; Iyengar, S. S.; Stevens, P. S. Experimental and Ab Initio Dynamical Investigations of the Kinetics and Intramolecular Energy Transfer Mechanisms for the OH 1,3-Butadiene Reaction between 263 and 423 K at Low Pressure. *The Journal of Physical Chemistry A* **2008**, *112* (31), 7227–7237.

(45) Leszczyński Jerzy; Shukla, M. K. *Practical aspects of computational chemistry*; Springer: New York, 2016.

(46) Kaufman, J. J. *Quantum Chemical Investigations of the Mechanism of Cationic Polymerization and Theoretical Prediction of Crystal Densities and Decomposition Pathways of Energetic Molecules*; Defense Technical Information Center: Ft. Belvoir, 1987.

(47) Tironi, I. G.; Sperb, R.; Smith, P. E.; Gunsteren, W. F. V. A generalized reaction field method for molecular dynamics simulations. *The Journal of Chemical Physics* **1995**, *102* (13), 5451–5459.

(48) Kramer, C.; Spinn, A.; Liedl, K. R. Charge Anisotropy: Where Atomic Multipoles Matter Most. *Journal of Chemical Theory and Computation* **2014**, *10* (10), 4488–4496.

(49) Iyengar, S. S.; Schlegel, H. B.; Voth, G. A. Atom-Centered Density Matrix Propagation (ADMP): Generalizations Using Bohmian Mechanics†. *The Journal of Physical Chemistry A* **2003**, *107* (37), 7269–7277.

(50) Davidson, M. The origin of the algebra of quantum operators in the stochastic formulation of quantum mechanics. *Letters in Mathematical Physics* **1979**, *3* (5), 367–376.

(51) Buizza, R.; Milleer, M.; Palmer, T. N. Stochastic representation of model uncertainties in the ECMWF ensemble prediction system. *Quarterly Journal of the Royal Meteorological Society* **2007**, *125* (560), 2887–2908.

(52) Berendsen, H. J. C. Molecular Dynamics Simulations: The Limits and Beyond. *Computational Molecular Dynamics: Challenges, Methods, Ideas Lecture Notes in Computational Science and Engineering* **1999**, 3–36.

(53) Tsuneda, T. Quantum Chemistry. *Density Functional Theory in Quantum Chemistry* **2014**, 1–33.

(54) Wilson, Zachary Ryan, "Ab Initio Methyl Linoleate Bond Dissociation Energies: First Principles Fishing for Wise Crack Products" (2017). *MSU Graduate Theses*. 3109.

(55) Wilson, Z. R.; Siebert, M. R. Methyl Linoleate and Methyl Oleate Bond Dissociation Energies: Electronic Structure Fishing for Wise Crack Products. *Energy & Fuels* **2018**, *32* (2), 1779–1787.

(56) Bartell, L. S., The correct physical basis of protobranching stabilization. *The Journalof Physical Chemistry A* **2012,** *116* (42), 10460-2.

(57) McKee, W. C.; Schleyer, P., Correlation effects on the relative stabilities of alkanes. *Journal of the American Chemical Society* **2013**, *135* (35), 13008-14

(58) Wodrich, M. D.; Corminboeuf, C.; Schleyer, P. v. R., Systematic Errors in Computed Alkane Energies Using B3LYP and Other Popular DFT Functionals. *Organic Letters* **2006**, *8* (17), 3631-3634

(59) Zhao, Y.; Truhlar, D., The M06 suite of density functionals for main group thermochemistry, thermochemical kinetics, noncovalent interactions, excited states, and transition elements: two new functionals and systematic testing of four M06-class functionals and 12 other functionals. *Theoretical Chemistry Accounts* **2008**, *120* (1-3), 215-241

(60) Bakker, Michael, "Improving biodiesel through pyrolysis: Direct dynamics investigations into thermal decomposition of methyl linoleate" (2019). *MSU Graduate Theses*. 4530.

(61) Winter, M., University of Sheffield, and WebElements Ltd. Carbon: radii of atoms and ions. *WebElements Periodic Table " Carbon " radii of atoms and ions*.

(62) Archambault, D.; Billaud, F. Non alimentary rapeseed oil upgrading: a parametric study of methyl oleate pyrolysis. *Industrial Crops and Products* **1998**, *7* (2-3), 329–334 DOI: 10.1016/s0926-6690(97)00065-4.

(63) Chai, M. (2012). Thermal Decomposition of Methyl Esters in Biodiesel Fuel: Kinetics, Mechanisms and Products.

APPENDICES

Appendix A. Complete ensemble of all products formed

1. 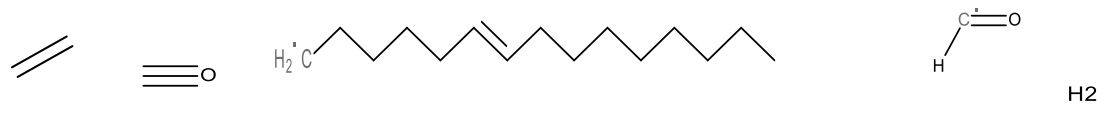

2. 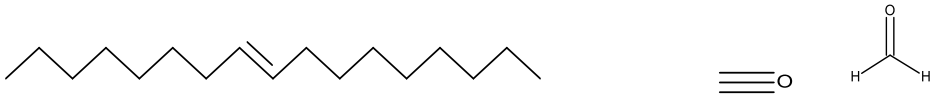

3. 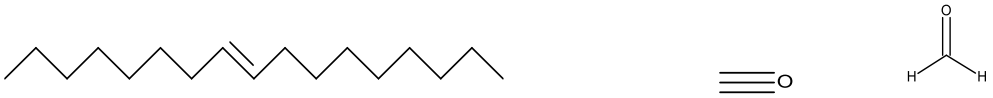

4. 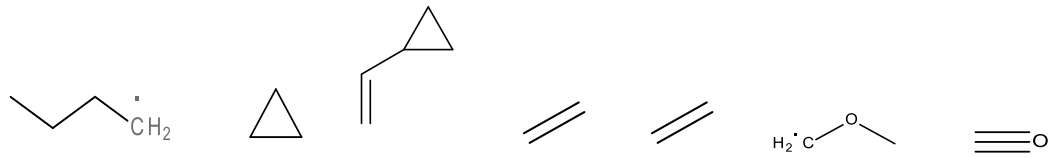

5. 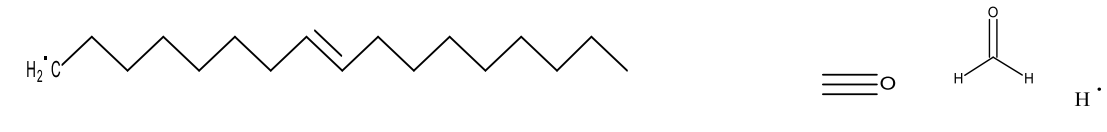

6. 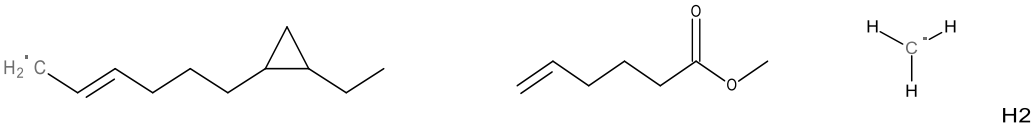

7. 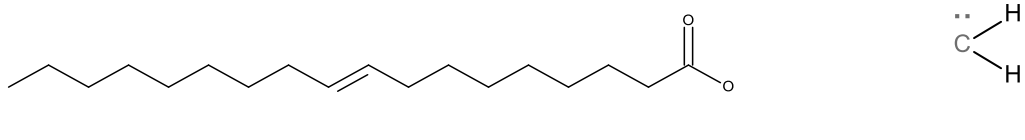

8. 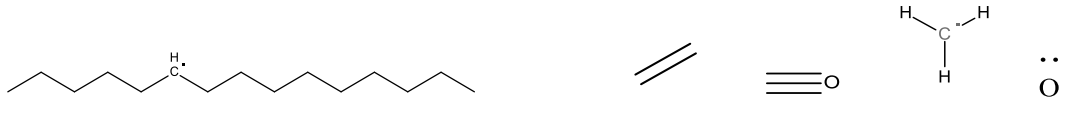

9. 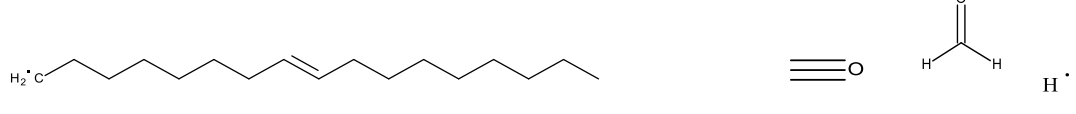

10. 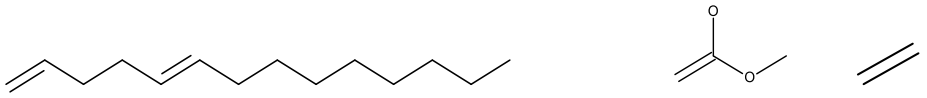

11. 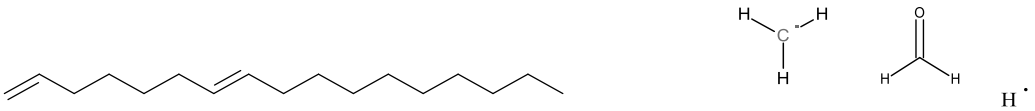

12. 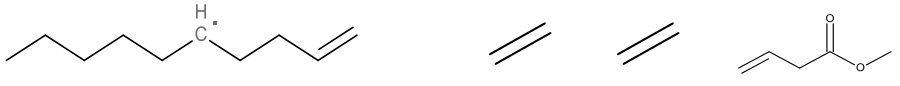

13. 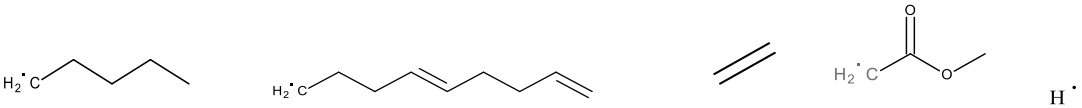

14. 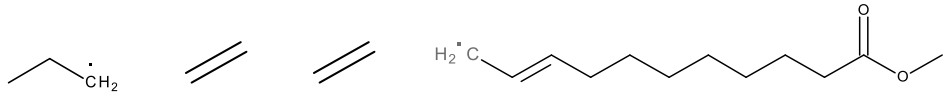

15. 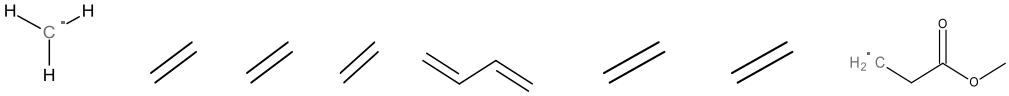

16. 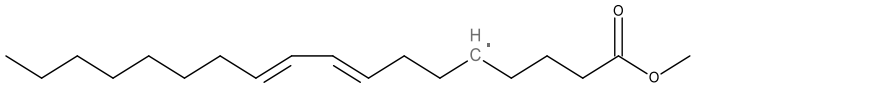

17. 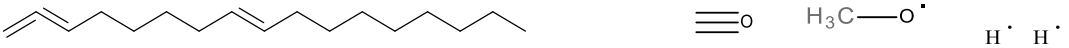

18. 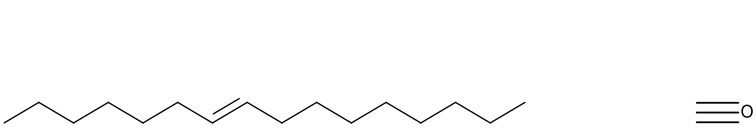

19. 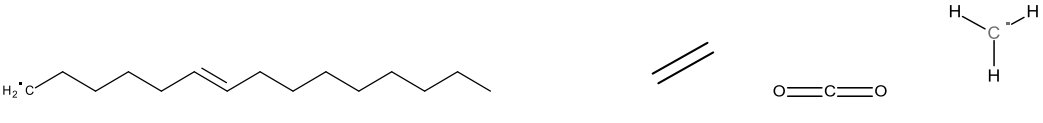

20. 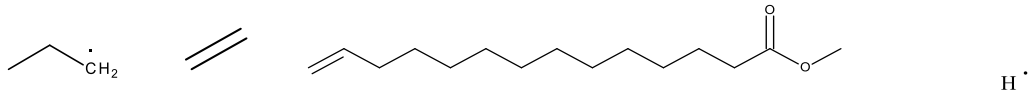

21. 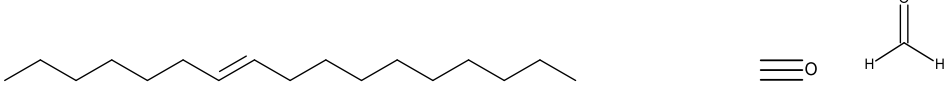

22. 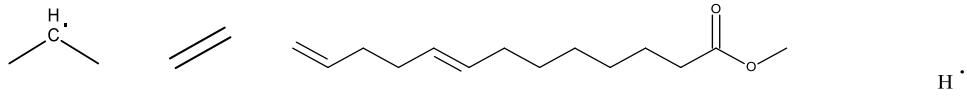

23. 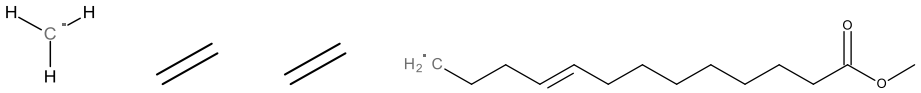

24. 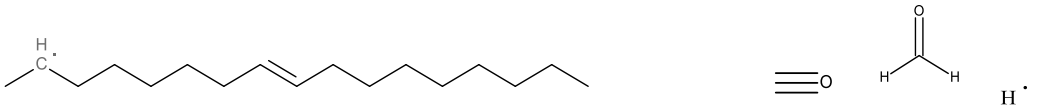

24. 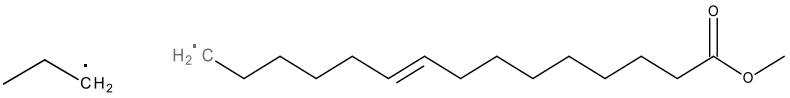

25. 

26. 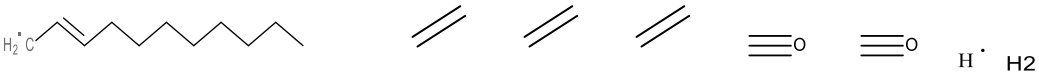

27. 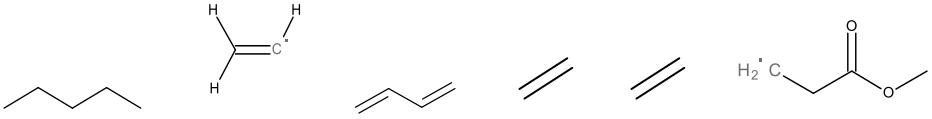

28. 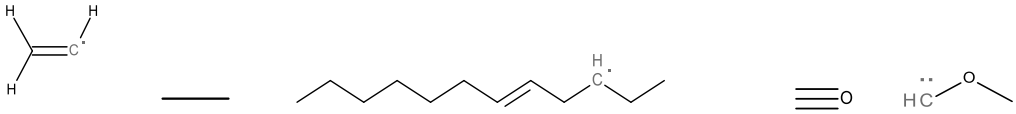

29. 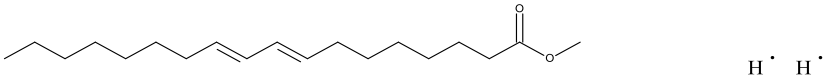

30. 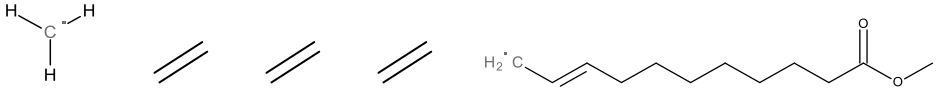

31. 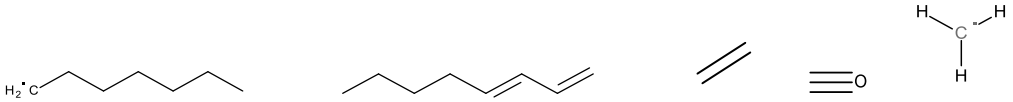

32. 

33. 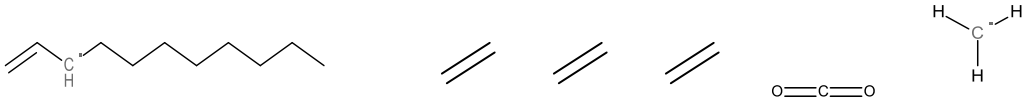

34. 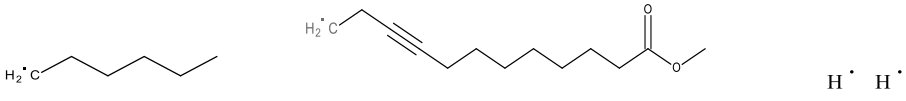

35. 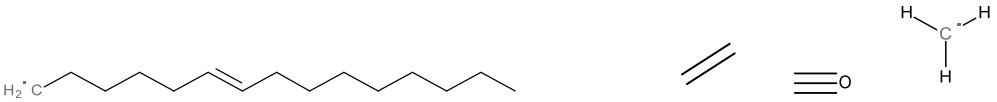

36. 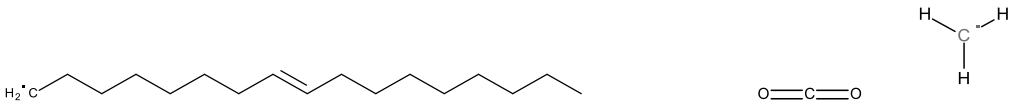

37. 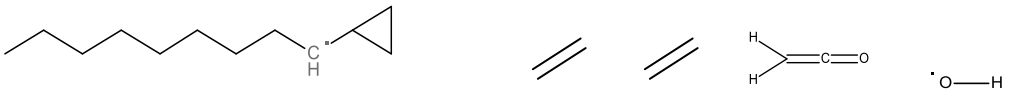

38. 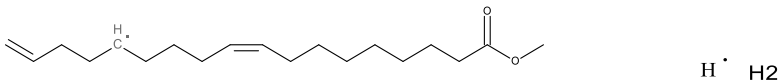

39. 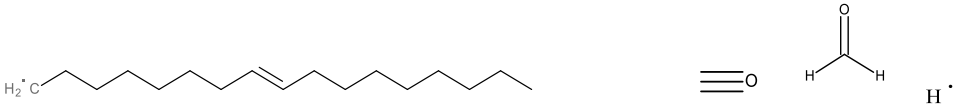

40. 

41. 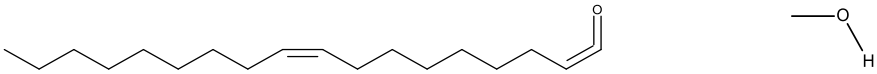

42. 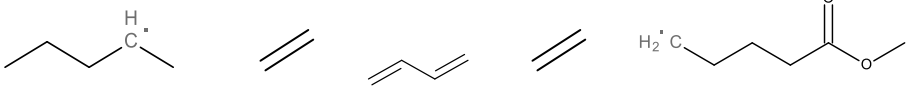

43. 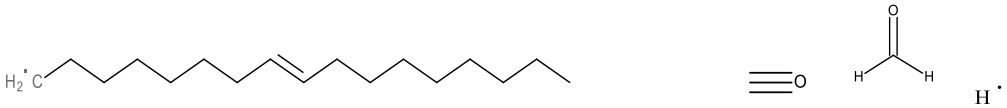

44. 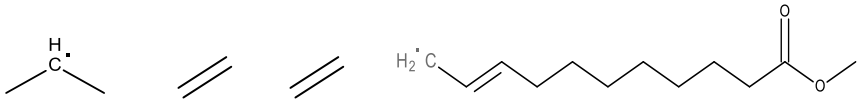

45. 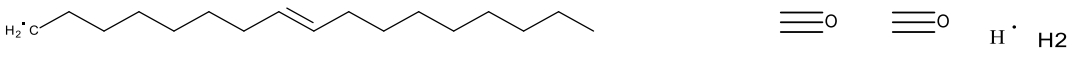

46. 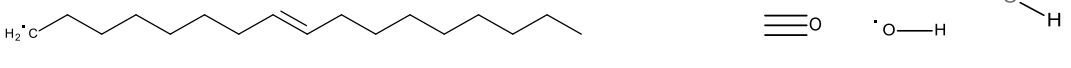

47. 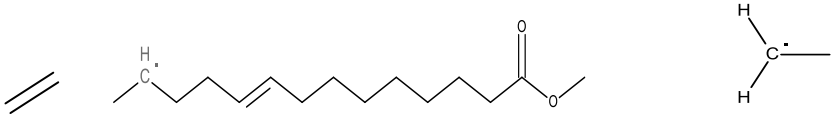

48. 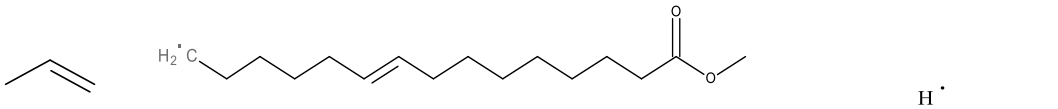

49. 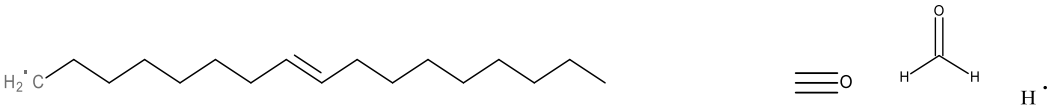

50. 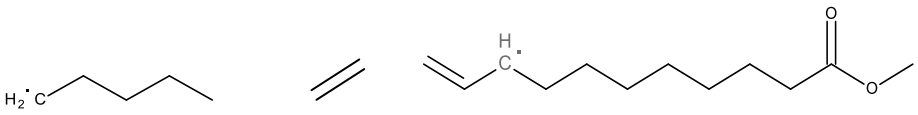

51 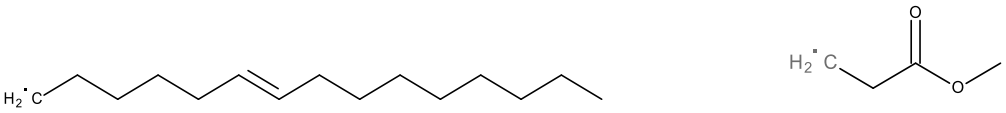

52. 

53. 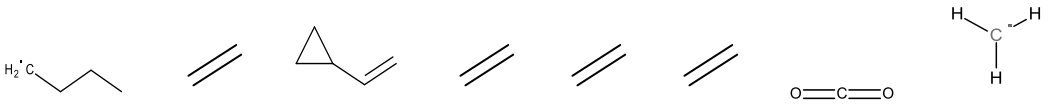

54. 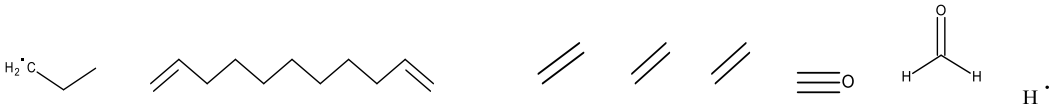

55. 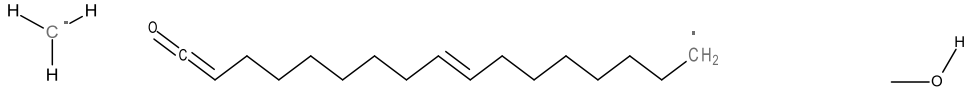

56. 

57. 

58. 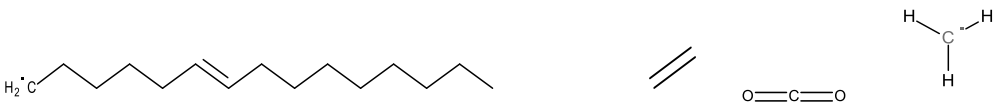

59. 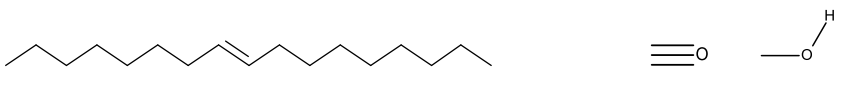

60. 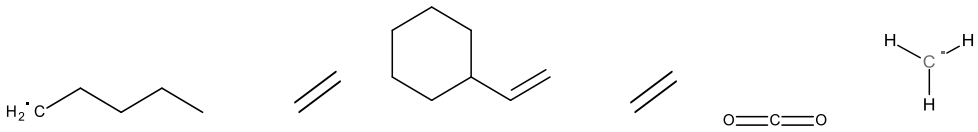

61. 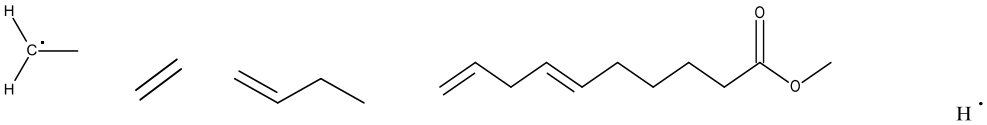

62. 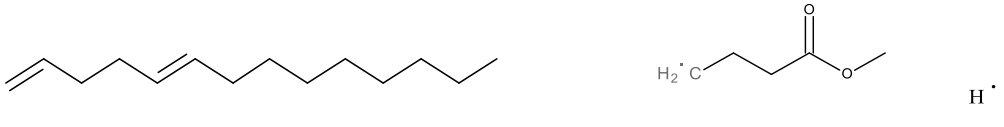

63. 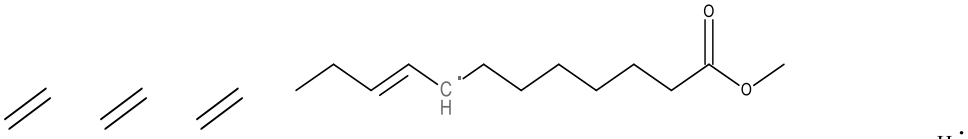

64. 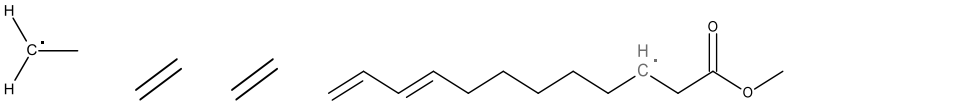

65. 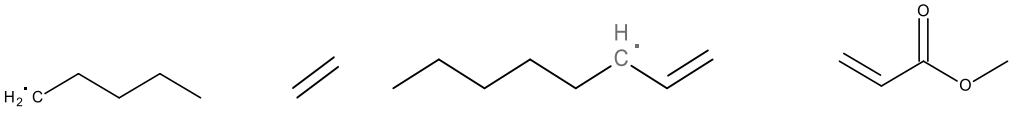

66. 

67. 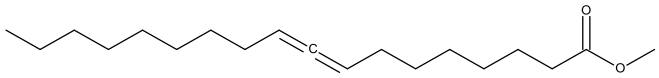

68. 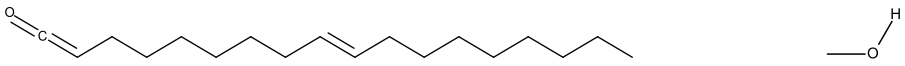

69. 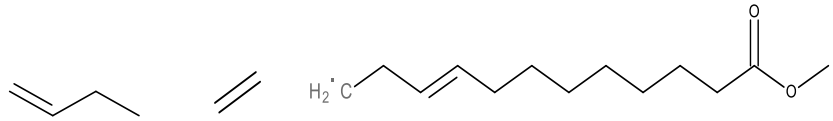

70. 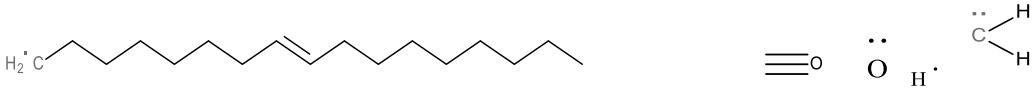

71. 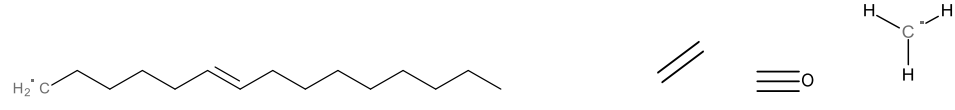

72. 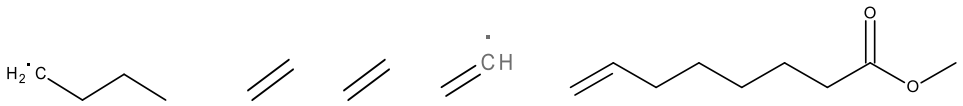

73. 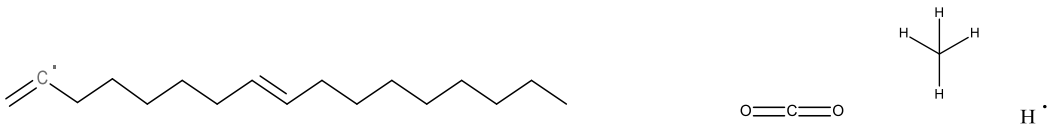

74. 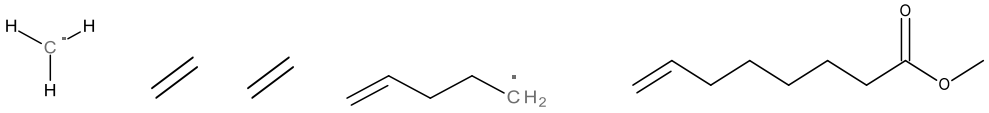

75. 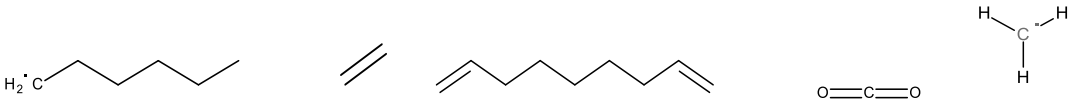

Appendix B. Energy data for all trajectories shown in appendix A

Reaction	ΔH (kcal/mol)	ΔG^{4000}(kcal/mol)	ΔS(kcal/mol/K)	ΔG^{673}(kcal/mol)
1	174.2	-415.6	0.12	92.5
2	39.1	-229.7	0.05	6.0
3	39.5	-216.9	0.06	-0.1
4	223.3	-634.6	0.20	90.6
5	143.4	-245.7	0.10	78.1
6	138.2	-279.8	0.13	48.7
7	92.3	-29.4	0.03	73.6
8	231.9	-329.9	0.09	169.4
9	143.3	-245.7	0.05	106.7
10	81.9	-160.6	0.13	-2.9
11	167.9	-364.2	0.13	77.1
12	177.4	-395.03	0.14	80.3
13	238.9	-368.03	0.11	165.9
14	129.6	-338.4	0.12	48.8
15	246.8	-803.2	0.24	85.3
16	161.2	-24.3	0.12	80.8
17	253.9	-238.6	0.06	214.0
18	105.9	-152.4	0.09	47.3
19	105.3	-275.4	0.09	46.2
20	154.8	-217.4	0.05	119.0
21	39.7	-194.5	0.10	-28.8
22	146.7	-280.9	0.11	74.8
23	143.4	-315.8	0.09	80.7
24	138.7	-251.4	0.10	71.4
25	90.4	-81.4	0.04	63.1
26	133.2	-396.8	0.12	51.6
27	206.9	-721.9	0.22	59.8
28	209.5	-536.8	0.17	92.1
29	243.1	-376.2	0.14	145.9
30	128.2	-71.3	0.05	94.0
31	159.2	-435.2	0.14	66.8
32	128.4	-419.7	0.13	44.2
33	134.1	-305.3	0.11	61.5
34	145.8	-525.2	0.15	42.6
35	259.3	-514.01	0.11	187.8
36	107.7	-499.1	0.08	54.6
37	83.7	-157.3	0.05	46.8
38	676.8	-415.5	0.16	566.8
39	124.7	-48.6	0.04	95.7
40	139.7	-220.3	0.09	82.0
41	157.2	-436.4	0.14	64.1
42	46.1	-98.6	0.03	23.8
43	172.9	-442.9	0.14	77.1

44	137.9	-210.2	0.08	82.2
45	127.4	-341.2	0.11	54.3
46	140.03	-371.9	0.12	56.8
47	604.9	-211.9	0.10	536.5
48	114.4	-177.9	0.07	68.8
49	211.4	-145.4	0.07	165.9
50	132.3	-237.3	0.09	73.0
51	104.3	-204.5	0.07	56.1
52	90.7	-37.7	0.03	70.8
53	130.1	-375.5	0.12	52.4
54	213.0	-752.0	0.14	116.7
55	243.8	-740.5	0.23	89.2
56	162.7	-269.2	0.11	88.0
57	125.4	-147.1	0.07	81.0
58	134.05	-321.03	0.11	62.3
59	107.7	-297.8	0.09	44.9
60	52.07	-198.5	0.05	17.3
61	125.002	-151.5	0.07	79.9
62	162.7	-393.8	0.13	74.6
63	169.5	-412.9	0.14	77.8
64	130.4	-324.9	0.11	59.7
65	212.4	-478.4	0.16	103.7
66	39.9	-88.3	0.03	19.1
67	46.6	-87.8	0.03	26.1
68	151.2	-277.3	0.10	82.5
69	316.4	-186.6	0.13	228.4
70	108.2	-290.9	0.09	46.5
71	182.3	-419.9	0.14	88.7
72	117.2	-228.8	0.08	62.6
73	171.6	-416.9	0.14	80.1
74	133.9	-413.8	0.13	49.3
75	164.8	-443.5	0.14	70.2